1958

Application of integral equation to the stability problem.

T Kusuda

Built-Up Members in Plastic Design

Progress Report No. 27

STRENGTH OF WIDE FLANGE BEAMS UNDER COMBINED INFLUENCE OF MOMENT, SHEAR AND AXIAL FORCE

by

Tadao Kusuda
Bruno Thürlimann

This work has been carried out as a part of an investigation sponsored jointly by the Welding Research Council and the Department of the Navy with funds furnished by the following:

American Institute of Steel Construction
American Iron and Steel Institute
Institute of Research, Lehigh University
Office of Naval Research (Contract No. 610(03))
Bureau of Ships
Bureau of Yards and Docks

Fritz Engineering Laboratory
Department of Civil Engineering
Lehigh University
Bethlehem, Pennsylvania

May 1958

Fritz Laboratory Report No. 248.1

(Not for Publication)

TABLE OF CONTENTS

ABSTRACT

In plastic design of steel structures, it is generally assumed that the influence of shear forces on the plastic moment is negligible. However, in some structures, for instance built-up members with cutouts or Vierendeel girders, high shear forces may be accompanied by high axial forces, causing an appreciable reduction of the full plastic moment of the cross-section. Therefore this influence on the plastic moment should be studied and if necessary taken into account.

Although there are several studies on the influence of shear or axial forces on the plastic moment little seems to be known about the combined effect of shear and axial forces.

It appears that plastic design of built-up members requires the solution of two problems, one to establish the interaction curves for the plastic moment under the influence of both shear and axial forces and second to develop a design procedure based on these interaction curves. In this paper the combined effect of shear and axial forces on the plastic moment is studied by using lower bound method in the plastic analysis. Interaction curves are presented using non-dimensionsl parameters. Tests on the influence of shear and axial forces were carried out which confirm the theoretical analysis. Finally a design procedure of a built-up beam with a cut-out was developed using an iteration method.

I. INTRODUCTION

1.1 Scope of Investigation

"Simple Plastic Theory" of steel structures is based on certain assumptions concerning the bending moment-curvature relationship of members. It is assumed to be linearly elastic up to the full plastic moment M_p. Thereafter rotation takes place at constant moment, i.e., the member acts as if it contained a hinge rotation under a restraining moment M_p. This concept of the formation and indefinite rotation of a plastic hinge in a member whenever the full plastic moment is maintained at a section is of fundamental importance in this theory. In fact, the simplicity of the plastic analysis is due entirely to this concept. However, it must be recognized that the full plastic moment of a given member is actually not a definite, constant quantity. This is partly so because the static yield stress on which it is based is dependent to some extent on the manner of loading and the previous loading history. The full plastic moment M_p is equal to the product $\sigma_y . Z$, where σ_y is the static yield stress and Z is the plastic section modulus whose value depends solely upon the geometry of the cross-section. Thus variations in the value of the full plastic moment M_p will occur whenever effects are brought into play which alter the value of the static yield stress. As is well known, the yield stress of structural steel is affected by the rate of loading, the temperature of the specimen, and also by strain aging. Fortunately, it appears that

these effects will usually be quite small. Other factors which affect the value of the full plastic moment are the presence of axial thrust and shear force. Since in applications of plastic analysis, plastic hinges and hence the plastic moment usually occur at positions where one or both of these influences are present, it is of considerable importance to be able to predict the changes in the value of the full plastic moment due to these causes. It will appear that in many practical cases the effects of axial thrust and shear force are very small. Therefore the practice of neglecting these influences can be justified. However, there are types of structures for which it is important to make a proper allowance for these effects. For instance, in built-up members with cutouts or Vierendeel girders, high shear forces may be accompanied by high axial forces, causing an appreciable reduction of the full plastic moment.

Horne[1] studied the effect of shear on the plastic moment, assuming an idealized stress-strain relationship for a perfectly plastic material. Starting from the maximum shear theory of yielding and the equation of equilibrium for a state of plane stress, he obtained the parabolic shear stress distribution in the central elastic core. The reduction of the plastic moment due to shear for the case of a cantilever I-beam becomes:

$$\frac{M_p - M_{ps}}{M_p} = \frac{\sqrt{1 + 1.774 \frac{Z}{t\ell^2}} - 1}{1.774 \frac{Z}{t\ell^2}}$$

where

M_p = full plastic moment of the section

M_{ps} = reduced plastic moment due to shear

t = web thickness

Z = plastic section modulus

ℓ = length of cantilever

From this analysis Horne derived the critical ratio $\ell/d_w = 0.632 \frac{Z}{td^2} - 0.176$ with ℓ equal to the cantilever length and d_w equal to the web depth. Under this condition shear yielding occurs along the neutral axis, the shear stress distribution being parabolic over the entire depth of the web. For example, for a 10WF29 this limiting value becomes $\ell/d_w = 0.62$. Finally he concluded that the reduction in the plastic moment due to shear is small except for very short beams. For instance, the reduction in the carrying capacity due to shear stress is about 3% for a wide flange beam with $\ell/d_w = 2.0$.

Fujita[2] followed this lower bound method to determine the effect of shear on the plastic moment for a cantilever with a rectangular cross-section. He used Mises' yielding condition. His results were modified for wide flange shapes with a parameter of area of flange over area of web ratio A_f/A_w in the lecture notes of summer course on plastic design[3]. In these lecture notes the critical value of ℓ/d_w for shear failure in the web was given by 1.82 for $A_f/A_w = 2.0$ (for instance, 10WF29). The reduction in full plastic moment can

be expressed as

$$\frac{M_{ps}}{M_p} = \frac{8}{9} \cdot \frac{t\ell^2}{Z} \cdot \left[\sqrt{1 + \frac{9}{4} \cdot \frac{Z}{t\ell^2}} - 1 \right]$$

where

M_{ps} = reduced plastic moment due to shear

t = web thickness

ℓ = length of cantilever beam

Z = plastic section modulus

For 10WF29,

$t = 0.289"$

$Z = 34.7"^3$

$d_w = 9.22"$

$\ell = 18.44"$ for $\ell/d_w = 2.0$

Therefore $\frac{M_{ps}}{M_p} = 0.850$ and the reduction is 15%. This result is quite different from Horne's result which is equal to 3% for this case.

On the other hand, Green[4], Leth[5], Onat[6] and Drucker[7] have studied the same problem by means of the upper and lower bound theorems, the true value lying between these two bounds. They proposed several types of velocity fields for upper bounds as well as the stress fields for lower bounds. For example, Drucker obtained the following expression for a rectangular section by using a lower bound

$$\frac{M_{ps}}{M_p} = 2 \left(\frac{\ell}{d}\right)^2 \left(1 - \cos \frac{d}{\ell}\right) \quad \text{for} \quad \frac{d}{\ell} \leq \frac{\pi}{2}$$

for $\ell/d = 2.0$

$$\frac{M_{ps}}{M_p} = 0.979$$

resulting into a reduction of 2.1%.

The effect of an axial force on the plastic moment have been also studied since Baker, Horne and Roderick in 1949. After Baker's study on this problem Ketter[8], Onat[9] have developed the effect of axial force on full plastic moment. The reduction of full plastic moment can be expressed as

$$\frac{M_{pc}}{M_p} = 1 - \frac{A^a}{4tZ} \left(\frac{T}{T_y}\right)$$

for the case of neutral axis in web

$$\frac{M_{pc}}{M_p} = \frac{A}{2Z} \left(1 - \frac{T}{T_y}\right) . \left[d - \frac{A}{2b} \left(1 - \frac{T}{T_y}\right) \right]$$

for the case of neutral axis in flange,

where

M_{pc} = reduced plastic moment due to thrust

T = axial force

$T_y = \sigma_y . A$

A = total cross-sectional area

b = width of flange

d = depth of beam

t = thickness of web

Z = plastic section modulus of wide flange shapes

Horne[10] investigated the effect of both shear and axial force on the plastic moment and proposed an interaction curve of moment, shear and thrust.

The objective of this paper is to evaluate the combined effects of shear and axial force on the plastic moment. Two approaches were studied in a theoretical analysis. A few tests were carried out under different ratios of shear and axial force in order to confirm the theoretical analysis. The two approaches mentioned above are as follows.

Approach (A):

The flanges are assumed to carry no shearing stress at all, the shearing stress in the web is assumed to be of uniform distribution. If strain-hardening takes place in the flange plates only, the difference in bending stresses acting on each side of a small element dx of a beam gives the magnitude of shearing stress in web. It is quite natural to assume that a certain length of beam reaches strain-hardening under the condition of a moment gradient as in the case of a cantilever beam, because the moment-curvature relationship has no flat part under a moment gradient. But the assumption of a uniform distribution of shearing stress along the depth of the beam is made merely to simplify the problem. There is no special reason for this assumption except that the shearing stress distribution in the web of a wide flange beam is rather flat compared to the one of a beam with rectangular cross-section. Once the magnitude of the shearing stress in terms

of the known quantities such as dimensions and load is determined, the Mises' condition of yielding gives the interaction curves between shear, axial force and reduced full plastic moment.

Approach (B):

Similar assumptions as in the previous approach (A) are made. The flanges carry no shearing stress and the shearing stress τ in the web is uniform. However, in this approach (B) the intensity of shearing stress is assumed to be equal to the mean value of V/A_w, where V is the shear force acting at the end of the cantilever and A_w is the area of the web. In the case of a cantilever beam subjected to bending as well as shear and axial force, the contribution of bending stress to the plastification of the cross-section is reduced by the presence of shear and axial force. For a short beam, the effect of the shear force is rather severe. Plastic failure will be caused mainly by shear rather than bending. This tendency of shear failure will be accelerated by the presence of an axial force. Therefore the shearing stress might be assumed to be of uniform distribution along the depth of the beam and its intensity equal to V/A_w as an extreme case of shear failure in a short beam. Tests confirm this possibility of uniform distribution of shear stress by the pattern of slip lines occurring at yielding.

II. DESCRIPTION OF TESTS

2.1 Test Program

Since the reduction of the full plastic moment due to shear is generally negligible when the ratio ℓ/d_w, length of beam divided by depth of the web, is greater than 4, the ratio ℓ/d_w of the test specimens was chosen such that a considerable reduction of the full plastic moment due to shear only could be expected from the tests. From the theoretical analysis of wide flange shapes, presented in the subsequent Chapter IV, the critical value for shear failure is given by $\ell/d_w = 1.85$, assuming that the values A_f/A_w and d_f/d_w of the wide flange shapes are equal to 2.0 and 1.05 respectively, where A_f stands for the total area of the upper and lower flange, A_w is the web area, d_f the distance of the center line of the two flanges, and d_w the depth of the web. This critical value may be affected by the presence of an axial force. Anticipating the results of the theoretical analysis the critical values ℓ/d_w for shear failure of a wide flange shape with $A_f/A_w = 2.0$ and $d_f/d_w = 1.05$ are reduced by an axial force T as follows:

T/T_y :	0	0.1	0.2	0.3	0.4	0.5
ℓ/d_w :	1.85	1.60	1.30	1.05	0.75	0.50

Hence, the critical ratio ℓ/d_w is inversely proportional to the ratio of axial force T/T_y, where T_y is equal to $\sigma_y A$, A being the total area of the cross-section. T_y is therefore

the axial force which produces yielding of the cross-section under axial force only. A considerable reduction of the plastic moment can be obtained when the ratio ℓ/d_w is close to the critical value for shear failure. However, the local disturbance of the stress distribution in the cross-section of the beam due to the application of loading may also affect the test result if the beam is quite short compared to its depth. According to St. Venant's principle this end effect can be neglected when the ratio ℓ/d_w is greater than 2.0. Therefore the length over depth ratio ℓ/d_w of the specimen was fixed at 2.0.

The particular set-up chosen is shown in Fig. 1. Axial tension was applied to the specimens in order to diminish the tendency of lateral buckling in the plastic range. The ratio of axial tension to shear, T/V, varies according to the length of the fixture as shown in Fig. 2. The ratio M_{pm}/M_p, where M_{pm} is the reduced plastic moment of the section, is also shown in Fig. 2 according to the length of the fixture. For test specimens No. 1, No. 2 and No. 3, the ratio T/T_y is 0.13, 0.19 and 0.37 respectively. It was determined analytically that the reduction in the plastic moment due to shear and thrust should be more than 30% for specimen No. 3 such that the test results should give a definite answer concerning the reliability of the theoretical analysis even if the results should be influenced by some experimental errors. The load P, axial tension T and shear V in Fig. 2 are computed using yield stress $\sigma_y = 36^{ksi}$.

2.2 Test Specimens

The wide flange shape 10WF29 was chosen for the test specimens because the ratios $A_f/A_w = 2.176$ and $d_f/d_w = 1.054$ are close to the mean values for wide flange shapes, $A_f/A_w = 2.0$ and $d_f/d_w = 1.05$ respectively. The length of the specimens is 18 1/2" so that the ratio $\ell/d_w = 2.0$. The specimens were welded to the flange plate of the wide flange shape 12WF58 by using a continuous fillet weld of 1/3" as shown in Fig. 1. The fixing beam 12WF58 was stiffened by means of vertical and diagonal stiffeners of 1/2" thick plate welded to the web plate.

After testing a specimen, the tested section was cut off by flame cutting and the new test section was welded to the fixing beam as shown in Fig. 1 by dotted lines.

Loading pins of 3" diameter were welded to the specimen and the fixture so that a tensile force could be applied by using a standard testing machine. Figure 1 illustrates the method of load application. Since the end of the test specimens were tapered and stiffened by means of a 3/4" thick plate the axial force could easily be transmitted to the flange plate of the specimen.

2.3 Test Set-Up

The instrumentation for these tests consisted of seven dial gages. Three of them were used for deflection measurements along the center line of the flange plate, two were

curvature gages and last two measured the rotation on both sides of the web plate as shown in Fig. 1. The deflections were measured at distances of 3 inches, 7 inches and 11 inches from the load point. The dial gage frame for the deflection measurement was welded to the stiffeners of the fixing beam so that the deformation due to warping at fixed end of the cantilever would not affect the base line of the dial gages (Photo 1). The gage length of the curvature gage was 1" and the measuring position was chosen as close as practical to the fixed end of the specimens because of the steep gradient of the applied moment. The total rotation angle was measured by means of the dial gages indicating the relative rotation between the flange plate of the fixture and a reference point on the web plate of the specimen. The gage length of the rotation gage was 11 1/2 inches. A screw type testing machine was used for the loading because of its accuracy and convenience for the deflection control in plastic range (Photo 2).

2.4 Test Procedure

The rate of application of load was about 0.03 inches per inch per minute in the plastic range and a short time (about 5 minutes) was taken to allow the load and strains to reach equilibrium at each step of loading. For the specimen No. 1 ($T/T_y = 0.13$), the first yield line started along the web center at a load equal to 66.3 kips. Yielding of the flange on tension side of the beam commenced at the load of

69.2^{kips}. The yield lines at the flange on compression side of the beam developed at load of 86.1^{kips}. Hence yielding in web due to shear and thrust preceded yielding in the flange plates due to bending and axial force. For specimen No. 2 ($T/T_y = 0.19$), initial yielding started similarly in the web plate at a load of 69.9^{kips} and yield line commenced in the flange on tension side of the beam at load of 99^{kips}. For specimen No. 3 ($T/T_y = 0.37$), the initial yield started at in web plate and the flange plate on tension side of the beam simultaneously. All specimens, No. 1 to No. 3, exhibited strain-hardening at once before the yielding spreaded over the specimens. This means that there is no flat portion neither in load-deflection nor moment-curvature diagrams of the specimens. As shown in Photo 3 neither lateral nor local buckling occurred in the plastic range before cracking started from the corner of the fillet welds between the flange plates of the specimens and the fixing beam. Although failure of each specimen took place by fracture of the welds, a considerable plastic deformation was obtained for each specimen in the strain-hardening range prior to crack initiation shown in Fig. 3. No sudden fracture of the brittle type occurred in any specimen.

2.5 Coupon Tests

To obtain the mechanical properties of the steel, two standard tensile specimens (ASTM A-359) from the flange plate and one from the web plate of the 10WF29 beam were prepared.

The specimens were tested in a hydraulic testing machine. Load and elongation over an 8 inch gage length were measured and plotted by means of an automatic stress-strain recorder. This instrument could record strains well into strain-hardening without resetting.

The rate of application of load was about 0.007 inches per inch per minute in the plastic range, a rate much lower than the usual standard mill test rate. This reduced rate of loading was used because the results were to be used to predict values for static tests where equilibrium of load and deformation would be obtained at each load increment before readings would be taken. A unique feature of these tests was the taking of "static yield load" readings in the yield range. After the yield region had been reached, but before strain-hardening had commenced, the strain rate was reduced to zero for a period of a few minutes to allow the load to reach an equilibrium point. Static readings were then taken. From this reading the lowest possible yield stress could be calculated.

2.6 Control Test

A length of the 10WF29 section was tested as a control beam to obtain moment-curvature relationship under pure bending. The specimen tested was 76 inches long with vertical stiffeners welded at support and load points to prevent web crippling (Fig. 10). A screw type universal testing machine was used

to apply load to the specimen supported on rollers on a 76 inch span. Loads were applied at the points 2 feet from the both ends of the beam using a spreader beam to distribute the testing machine load to two rollers.

The instrumentation used to measure the curvature in the constant moment region consisted of two dial gages recording bending strains over a 10 inch gage length and a dial indicator, recording center deflection.

Load was applied continuously at a moderate rate which allowed gage readings to be taken without interrupting the loading. After the plastic range had been reached, it was necessary to halt the application of load twice to allow resetting of the dial indicators. Loading was continued until the ultimate load was reached, after considerable strain-hardening followed by a gradual drop in load due to instability of the compression flange.

III. RESULTS OF TESTS

3.1 Determination of Modified Plastic Moment, M_{pm}

If a beam is subjected to a constant moment over part of its length the load-deflection or moment-curvature diagram shows a definite flat portion in the plastic range. However, under a moment gradient no such flat portion exists. Therefore a criterion must be chosen to determine the plastic moment. The following method was used. The load deflection

curves, such as shown in Fig. 3, show a definite break. For small loads the specimens exhibited purely elastic behavior. After yielding the increase in deflection is very much accelerated. The point of intersection of the tangents to the elastic and strain-hardening part of the curve determines a load P_u. Beyond this load large plastic deformations take place and a hinge develops without too significant an increase in load. Hence, the moment corresponding to this load is taken equal to the plastic moment M_{pm}. By static for the cantilever specimens it follows $M_{pm} = P_u \ell$.

Similarly the value of M_{pm} can be obtained from a moment-curvature diagram of a beam under moment gradient. The intersection of the tangents drawn to the elastic and strain-hardening part determines M_{pm} as shown in Fig. 6.

Finally, the theoretical "failure" load P_u is defined similarly as the point at which the rotation of the equivalent hinge takes place rapidly in the beam under moment gradient as shown in Fig. 7. The values of M_{pm} obtained from deflection, curvature and rotation measurements are described in the following part and compared to the theoretical values.

(a) M_{pm} obtained from Load-Deflection Curves

Figure 3 shows the load-deflection curves for each specimen No. 1, 2 and 3 corresponding to the condition T/T_y equal to 0.13, 0.19 and 0.37 respectively. The deflection was measured 3 inches from the loading point. Figure 4 and 5 show

the load-deflection curves for deflections measured at 7 and 11 inches from the loading point respectively. The dashed lines in Fig. 3 represent the theoretical load-deflection curve. If this curve differs from the tangent to the strain-hardening part a dotted line was drawn to the experimental curve in order to determine P_u or M_{pm}. The loads P_u determined from the different load-deflection curves measured at 3, 7 and 11 inches from the loading give fair correlation. The results are summarized in Table I. The maximum test loads were reached at the initiation of a crack in the welds.

(b) Moment-Curvature Curves

The moment-curvature diagram of each specimen is shown in Fig. 6. From these curves the reduced plastic moment M_{pm} was derived as 1030 kips-inches, 1040 kips-inches and 860 kips-inches for specimen No. 1, 2 and 3 respectively. The corresponding loads P_u are obtained by dividing M_{pm} by the length of the cantilever beam, hence P_u equals 70 kips, 85 kips and 126 kips respectively. The rotations at maximum moment are dependent on the T/T_y ratio as may be seen from Fig. 6. The specimen No. 1 ($T/T_y = 0.13$) shows the largest rotation among the three specimens. The curvatures at maximum moment for each specimen reached 2.15 radian/in., 1.87 radian/ in., and 0.7 radian/in. for No. 1, No. 2 and No. 3 respectively.

(c) Hinge Rotation Curves

Load-hinge rotation curves are shown in Fig. 7. Since the hinge rotation is defined as the inelastic rotation taking place within a certain length of beam, no rotation takes place below the proportional limit. Therefore the load P_u from the rotation curves can be obtained by the intersection between tangent to that curve in the strain-hardening range and the vertical axis of load in Fig. 7. The hinge rotation is given by

$$\theta_p = \frac{\Delta - \delta_{RP}}{\text{Gage Length of Rotation Gage}} - \theta_e$$

where

$$\theta_e = \frac{V}{2EI}(\ell^2 - x^2)$$

θ_e = corresponding angle rotation resulted from a deflection due to shear force

V = shear force at the end of a cantilever beam

ℓ = length of a beam

x = distance from free edge of a beam

Δ = deflection of a beam at a reference point of the rotation gage

δ_{RP} = reading of a dial gage for rotation measurement

The above expression is explained as follows. The deflection due to shear indicates a certain amount of reading on the rotation gage. But this rotation must be subtracted from the test result as indicated in Fig. 8. From Fig. 7, the load P_u

is given by 70 kips, 82 kips and 120 kips respectively.

Finally, the values P_u obtained by different methods of measurement are compared to each other and to theoretical predictions as shown in Table I. From this Table I, P_u can be determined as

T/T_y	0.13	0.19	0.37
P_u	70kips	82kips	126kips

3.2 Lateral Rotation

The difference in readings of the two rotation gages mounted on both sides of the web plate gives the lateral rotation. The development of lateral rotation indicates the initiation of lateral or local buckling. These values are plotted on Fig. 9 for each specimen. Specimen No. 1 has developed considerable lateral rotation compared to the other two specimens. However, no evidence of lateral buckling was noticed as seen in Photo 3. Specimen No. 2 rotated to one side up to a certain load and then turned back to the reverse side because of a slight initial distortion due to fillet welding. Figure 9 shows that the maximum loads are given by neither lateral nor local buckling but the initiation of crack at fillet welds for these special cases. The width over thickness ratio of the flange plate is 11.6 for a 10WF29. This value is much less than the critical ratio 17 for the local buckling of a flange plate in strain-hardening range. The maximum unbraced length to prevent the lateral buckling in plastic range under moment gradient

is approximately given by the following expression.

$$\frac{1}{C_f}(L/r_{yy}) = 48 \text{ for the moment ratio } \rho = \frac{M}{M_p} = 0$$

where

C_f = restraint factor = 1.0 for simply supported ends

r_{yy} = radius of gyration about weak axis

r_{yy} = 1.34 inches for 10WF29

Therefore $L \geq 64.5$ inches

Since the length of the specimen is only 18.5 inches and the maximum unbraced length is larger than 64.5 inches for this case, then no lateral buckling could happen in these tests. The local buckles on the compression side at the fixed end of the beam as evident in Photo 3 for specimen No. 1 and No. 2 occurred after considerable cracking along the fillet welds had developed.

3.3 Maximum Load

As mentioned in the previous section the maximum loads for these test specimens were reached at the initiation of crack along the welds. The values of maximum loads are given in the following table. Also shown are the corresponding nominal stresses computed by means of conventional methods using the values of $I = 374^{in\,4}$ and $A = 20.5^{in\,2}$ for 1/3 inch fillet welds.

T/T_y	0.13	0.19	0.37
P_{max}	117 kips	137 kips	181 kips
T_{max}	71 kips	104 kips	169 kips
V_{max}	95 kips	91 kips	65 kips
M_{max}	1760k-inches	1680k-inches	1200k-inches
σ_{bend}	35.6ksi	34.1ksi	24.6ksi (at throat)
$\sigma_{tension}$	4.9ksi	7.1ksi	11.7ksi (at throat)
σ_{total}	40.5ksi	41.2ksi	36.3ksi (at throat)
$\tau_{av.}$	6.5ksi	6.3ksi	4.5ksi (at throat)
$\tau_{av.\ web}$	35.8ksi	34.2ksi	24.4ksi (at web)

These stresses are average stresses at the throat. Assuming stress concentration factor of say 1.5, the stresses reached approximately 60ksi. This value corresponds approximately to the ultimate tensile strength of a weld produced by an ordinary E 6000 type electrode. The average shearing stress of the flange fillets was quite small compared to the ones of the web plate where the shearing stress is beyond the yield stress under pure shear.

3.4 Results of Coupon and Control Tests

a) Coupon Test

The area-mean values of Young's modulus E, strain-hardening modulus E_{st} and static yield level σ_y computed from

the results of the coupon tests were as follows:

$$E = 29{,}000^{ksi}$$
$$E_{st} = 900^{ksi}$$
$$\sigma_y = 37^{ksi}$$

b) Control Test

The moment-curvature relationship of the control beam under uniform moment is shown in Fig. 10. The upper part of this figure gives an enlarged portion of the diagram in order to indicate more clearly the flat portion of this diagram and the value of full plastic moment M_p. This value of the full plastic moment obtained from the control test is 1,240 k-inches. It was used as the standard value to compute the reduction in full plastic moment due to shear and axial force. The value of full plastic moment computed by means of the plastic modulus Z for a 10WF29 and the static yield stress obtained from coupon tests is

$$M_p = \sigma_y Z = 37 \times 34.7 = 1284 \text{ kip-inches}$$

Hence, the value obtained from the control test is 3.5% less than the calculated one. This difference is due mostly to the difference between the actual dimensions of wide flange section on the handbook (AISC) values.

IV. THEORETICAL ANALYSIS

4.1 Determination of Modified Plastic Moment M_{pm} Under Moment, Shear and Axial Forces

In general exact solutions of problems involving plasticity are not possible. However, two powerful tools are available to estimate the carrying capacity. It has been demonstrated[11] that a solution satisfying equilibrium conditions gives a lower bound of the carrying capacity, thus producing a safe estimate even if a corresponding mechanism does not develop. A solution which concentrates on the collapse mode, or a possible velocity field gives an upper bound for the collapse load. Here, a lower bound solution is discussed and two approximations are proposed.

a) Lower Bound Method

A lower bound requires that the stress distribution in wide flange section satisfies the condition of equilibrium and also the boundary conditions. Under certain limitations of the magnitude of shear and axial force, the stress distribution is assumed to be the same as that in a beam with rectangular cross-section. As shown by Prager and Hodge[11], and also by Horne[1], under the simplifying assumptions which have been made the shear stress τ must be zero in the outer plastic regions, where the normal stress is σ_y. The corresponding stress distribution is shown in Fig. 11. This stress distribution seems to be reasonable as long as the axial force

T is small and the neutral axis is located in the web. Under these conditions the shearing stress distribution is parabolic and also symmetric about neutral axis. From Fig. 11, the moment at section A-A is given by:

$$M = \sigma_y \cdot \frac{A_f}{2} \cdot d_f + \sigma_y \cdot w \cdot \left[\left(\frac{d_w}{2}\right)^2 - \frac{1}{3} y_o^2 - \eta_o^2 \right] = V \cdot X \tag{1}$$

and the axial force T by:

$$T = \sigma_y \cdot w \cdot (2\eta_o)$$

With:

$$T_y = \sigma_y \cdot (A_w + A_f)$$

where

σ_y = static yield stress, the value of η_o is:

$$\eta_o = \frac{A_w + A_f}{2w} \quad \frac{T}{T_y} \tag{2}$$

Substituting Eq. (2) into (1),

$$V \cdot X = \sigma_y \frac{1}{2} \left[A_f d_f + \frac{1}{4} A_w d_w - \frac{1}{4} \cdot \frac{(A_f + A_w)^2}{w} \cdot \left(\frac{T}{T_y}\right)^2 - \frac{1}{3} w y_o^2 \right] \tag{3}$$

In the elastic portion of the web, the normal stress σ varies linearly:

$$\sigma = \sigma_y \cdot \frac{y}{y_o}$$

and

$$\frac{d\sigma}{dx} = -\sigma_y \cdot \frac{y}{y_o^2} \cdot \frac{dy_o}{dx}$$

The shearing stress in the web is determined by the equation of equilibrium:

$$\frac{\partial \sigma}{\partial x} + \frac{\partial \tau}{\partial y} = 0$$

or

$$\frac{\partial \tau}{\partial y} = -\frac{\partial \sigma}{\partial x} = \sigma_y \cdot \frac{y}{y_o^2} \cdot \frac{dy_o}{dx}$$

Taking the proper boundary conditions into account

$$\tau = \frac{1}{2} \sigma_y \left[\left(\frac{y}{y_o} \right)^2 - 1 \right] \cdot \frac{dy_o}{dx} \qquad (4)$$

Differentiating Eq. (3) with respect to x, an expression for the derivative $\frac{dy_o}{dx}$ is obtained

$$V = -\frac{2}{3} w\, y_o \sigma_y \cdot \frac{dy_o}{dx}$$

or

$$\frac{dy_o}{dx} = -\frac{3}{2} \cdot \frac{V}{w y_o \sigma_y} \qquad (5)$$

Substituting this expression into Eq. (4) gives:

$$\tau = \frac{3}{4} \cdot \frac{V}{w y_o} \left[1 - \left(\frac{y}{y_o} \right)^2 \right] \qquad (6)$$

According to this equation the shear reaches a maximum for $y = 0$ (neutral axis). From the limiting value of $\tau = \tau_y$

determined from Mises' yield condition,

$$\tau_y = \frac{\sigma_y}{\sqrt{3}} \tag{7}$$

for yielding under pure shear. Introducing this value into Eq. (6) the distance y_o is found

$$y_o = \frac{3\sqrt{3}}{4} \cdot \frac{V}{\sigma_y w}$$

Combining Eq. (8) with Eq. (3) an expression for the maximum moment at $x = \ell$ can be derived.

$$\frac{9}{16} \cdot \frac{M_{pm}^2}{\sigma_y w \ell^2} = M_p - \frac{1}{4} \cdot \frac{\sigma_y}{w} \cdot (A_f + A_w)^2 \cdot \left(\frac{T}{T_y}\right)^2 - M_{pm}$$

where $M_{pm} = V \cdot \ell$ = reduced plastic moment

or

$$\left(\frac{M_{pm}}{M_p}\right)^2 + \frac{16}{9} \cdot \frac{w\ell^2}{Z} \cdot \left(\frac{M_{pm}}{M_p}\right) - \left[\frac{16}{9} \cdot \frac{w\ell^2}{Z} - \frac{4}{9} \cdot \frac{\ell^2 (A_f + A_w)^2}{Z} \cdot \left(\frac{T}{T_y}\right)^2\right] = 0$$

where

$$Z = \frac{1}{2} A_f d_f + \frac{1}{4} A_w d_w = \text{plastic modulus of WF shapes}$$

$$\therefore \quad \frac{M_{pm}}{M_p} = \frac{8}{9} \xi \left[\sqrt{1 + \frac{9}{4\xi} - \frac{9}{16}\zeta^2} - 1\right] \tag{9}$$

where

$$\xi = \frac{wl^2}{Z} \quad \text{and} \quad \zeta = \frac{T}{w \cdot \ell \cdot \sigma_y}$$

Therefore, the reduction in full plastic moment due to shear and axial forces is given by Eq. (9). However, this equation is derived from an assumed stress distribution as shown in Fig. 11. The applicability of this Eq. (9) is obviously given by:

$$\eta_o + y_o \leqq \frac{d_w}{2}$$

From Eq. (2) and (8)

$$\frac{A_w + A_f}{2w} \cdot \frac{T}{T_y} + \frac{3\sqrt{3}}{4} \cdot \frac{V}{\sigma_y w} \leqq \frac{d_w}{2}$$

or

$$\left(1 + \frac{A_f}{A_w}\right) \cdot \frac{T}{T_y} + \frac{3}{2} \cdot \frac{V}{V_y} \leqq 1 \qquad (10)$$

where

$$V_y = \tau_y A_w = \frac{\sigma_y}{\sqrt{3}} \cdot A_w$$

The reduction in the full plastic moment within the limitation of Eq. (10) is shown in Fig. 12 by means of the non-dimensional parameters ξ and η. As may be seen the interaction curves between the reduced plastic moment, shear and axial forces are limited to a small range of axial force. It is therefore necessary to assume a different type of stress distribution in wide flange shapes imposing less restrictions to cover practical cases.

As proposed by Heyman and Dutton[12] an empirical distribution of σ and τ at the cross-section where a plastic hinge occurs, can be assumed to consist of a constant shear stress τ and a constant longitudinal normal stress throughout the web, together with zero shear stress and a uniform longitudinal normal stress σ_y in the flanges. In addition, it is assumed that σ and τ satisfy the Mises' yield condition,

$$\sigma^2 + 3\tau^2 = \sigma_y^2 \qquad (11)$$

In the following two possible approaches are outlined. Their applicability will be tested by comparison with experimental results.

b) Approximate Approach (A)

A stress distribution at the fixed end of the cantilever beam is assumed as shown in Fig. 13. The normal stress in the flange plates reaches σ_y, the flanges being assumed to carry no shearing stress. The normal stress in the web is $\xi\sigma_y$ where ξ is a non-dimensional factor less than unity. Its value is determined from the condition that the combination of the normal stress $\xi\sigma_y$ and the shearing stress τ fulfills Mises' yield condition. If it is assumed that the distribution of the flange stresses varies linearly over an infinitesimal beam length dx where the plastic hinge forms the magnitude of the shearing stress τ is determined as follows (see Fig. 13).

$$\frac{A_f}{2}\left(\frac{x}{\ell}+\frac{dx}{\ell}\right)\sigma_y = \frac{A_f}{2}\cdot\frac{x}{\ell}\cdot\sigma_y + \tau w\,dx$$

or

$$\tau = \frac{A_f}{2w\ell}\cdot\sigma_y \tag{12}$$

Introducing into the yield condition, Eq. (11), the normal stress $\xi\sigma_y$ and the above determined shearing stress fixes the value of ξ:

$$\xi = \sqrt{1 - 3\left(\frac{A_f}{2w\ell}\right)^2}$$

Using this value, the reduced plastic moment is given by the following expression

$$\frac{M_{pm}}{M_p} = 1 - \frac{1}{4}\frac{A_w d_w}{Z}\cdot\left[1-\sqrt{1-3\left(\frac{A_f}{2w\ell}\right)^2}\right] - \frac{(A_f+A_w)^2}{4wZ\sqrt{1-3\left(\frac{A_f}{2w\ell}\right)^2}}\cdot\left(\frac{T}{T_y}\right)^2 \tag{13}$$

This equation holds as long as the neutral axis is located within the web, the limiting value being:

$$\xi = \left(1+\frac{A_f}{A_w}\right)\cdot\frac{T}{T_y}$$

then

$$\frac{\ell}{d_w} = \sqrt{3}\cdot\frac{A_f}{A_w}\cdot\frac{1}{\sqrt{1-\left(1+\frac{A_f}{A_w}\right)^2\cdot\left(\frac{T}{T_y}\right)^2}} \tag{14}$$

and

$$\frac{M_{pm}}{M_p} = \frac{2\cdot\frac{A_f d_f}{A_w d_w}}{1+2\cdot\frac{A_f d_f}{A_w d_w}}$$

For the case in which the neutral axis falls within the flange plate, that is,

$$\frac{M_{pm}}{M_p} < \frac{2\,\frac{A_f d_f}{A_w d_w}}{1 + 2\frac{A_f d_f}{A_w d_w}}$$

the reduction in the plastic moment is given by

$$\frac{M_{pm}}{M_p} = \frac{4\left(\frac{d_f}{d_w}\right)\left[\frac{A_f}{A_w} - \left(1+\frac{A_f}{A_w}\right)\frac{T}{T_y}\right]}{\left(1+2\frac{A_f d_f}{A_w d_w}\right)\left[1+3\left(\frac{d_f}{2\ell}\right)^2\right]} \times$$

$$\times\left[1 + \frac{\sqrt{1+3\left(\frac{d_f}{2\ell}\right)^2\left[1-\left\{\frac{A_f}{A_w}-\left(1+\frac{A_f}{A_w}\right)\left(\frac{T}{T_y}\right)\right\}^2\right]}}{\frac{A_f}{A_w} - \left(1+\frac{A_f}{A_w}\right)\cdot\frac{T}{T_y}}\right] \qquad (15)$$

Finally, if shear failure governs:

$$\frac{M_{pm}}{M_p} = \frac{2}{\sqrt{3}}\cdot\frac{\ell}{d_w}\cdot\frac{\sqrt{1-\left(1+\frac{A_f}{A_w}\right)^2\cdot\left(\frac{T}{T_y}\right)^2}}{1+2\cdot\frac{A_f d_f}{A_w d_w}} \qquad (16)$$

Equations (13), (14), (15) and (16) are plotted in Fig. 13 by using the values of

$$\frac{A_f}{A_w} = 2.0 \quad \text{and} \quad \frac{d_f}{d_w} = 1.05$$

c) Approximate Approach (B)

If a cantilever beam is quite short, for instance $\ell/d_w \leqq 2.0$, then the plastification of the built-in end will

be produced primarily by shear yielding rather than bending. The presence of axial force accelerates the initiation of yielding. The simplest assumption concerning a distribution of shearing stress is to postulate a uniform stress τ over the web, or:

$$\tau = V/A_w \tag{17}$$

where V = shear force at end of cantilever

A_w = area of web

The magnitude of axial force T is given using a notation illustrated in Fig. 14 (a)

$$T = \eta_o A_w \xi \sigma_y \tag{18}$$

where $\xi \sigma_y$ = normal stress in web

$$0 < \eta_o < 1$$

The Mises' yield condition is fulfilled if

$$(\xi \sigma_y)^2 + 3\tau^2 = \sigma_y^2 \tag{19}$$

or

$$\xi^2 + 3\left(\frac{\tau}{\sigma_y}\right)^2 = 1$$

From Eq. (18),

$$\xi = \frac{T}{\eta_o A_w \sigma_y} = \frac{1}{\eta_o} \cdot \left(1 + \frac{A_f}{A_w}\right) \cdot \frac{T}{T_y}$$

and from Eq. (17)

$$\frac{\tau}{\sigma_y} = \frac{V}{A_w \sigma_y} = \frac{1}{\sqrt{3}} \cdot \frac{V}{V_y}$$

Substituting these expressions for ξ and τ/σ_y into Eq. (19), then

$$\eta_o = \frac{(1 + \frac{A_f}{A_w}) \cdot \frac{T}{T_y}}{\sqrt{1 - (\frac{V}{V_y})^2}} \qquad (20)$$

For the limiting case, $\eta_o = 1$, the corresponding moment is

$$M_{pm} = V \cdot \ell = \sigma_y \cdot \frac{A_f}{2} \cdot d_f$$

$$\therefore \quad V = \frac{M_{pm}}{\ell} = \frac{\sigma_y A_f d_f}{2\ell}$$

$$\therefore \frac{V}{V_y} = \sqrt{3} \cdot \frac{A_f}{A_w} \cdot \frac{d_f}{\ell}$$

From Eq. (20),

$$\frac{\ell}{d_f} = \frac{\sqrt{3} \cdot \frac{A_f}{A_w}}{\sqrt{1 - (1 + \frac{A_f}{A_w})^2 \cdot (\frac{T}{T_y})^2}}$$

and

$$\frac{M_{pm}}{M_p} \geq \frac{2 \frac{A_f d_f}{A_w d_w}}{1 + 2 \frac{A_f d_f}{A_w d_w}} \qquad (21)$$

In this range, the neutral axis is located in the web and the reduced plastic moment M_{pm} can be expressed as

$$M_{pm} = \sigma_y \cdot \frac{A_f}{2} \cdot d_f + \frac{1}{4} \xi \sigma_y A_w d_w (1 - \eta_o^2)$$

From Eq. (20)

$$\eta_o^2 = \frac{(1 + \frac{A_f}{A_w})^2 \cdot (\frac{T}{T_y})^2}{1 - (\frac{V}{V_y})^2}$$

and

$$\xi = \sqrt{1 - (\frac{V}{V_y})^2}$$

$$M_{pm} = V\ell = \frac{1}{\sqrt{3}} \sigma_y A_w \ell \cdot \frac{V}{V_y}$$

Therefore

$$\frac{4}{\sqrt{3}} \cdot \frac{\ell}{d_w} \cdot \frac{V}{V_y} - 2 \frac{A_f d_f}{A_w d_w} = \sqrt{1 - (\frac{V}{V_y})^2} - \frac{(1 + \frac{A_f}{A_w})^2 \cdot (\frac{T}{T_y})^2}{\sqrt{1 - (\frac{V}{V_y})^2}}$$

or

$$\frac{9}{16}(1 + 2\frac{A_f d_f}{A_w d_w})^4 \cdot (\frac{M_{pm}}{M_p})^4 \cdot (\frac{d_w}{2\ell})^4 - \frac{3}{4}(1 + 2\frac{A_f d_f}{A_w d_w})^2 (\frac{M_{pm}}{M_p})^2 \times$$

$$\times \left[2\{1 - (1 + \frac{A_f}{A_w})^2 (\frac{T}{T_y})^2\} - \{(1 + 2\frac{A_f d_f}{A_w d_w})(\frac{M_{pm}}{M_p}) - 2\frac{A_f d_f}{A_w d_w}\}^2 \right] \cdot (\frac{d_w}{2\ell})^2$$

$$+ \left[\{1 - (1 + \frac{A_f}{A_w})^2 (\frac{T}{T_y})^2\}^2 - \{(1 + 2\frac{A_f d_f}{A_w d_w})(\frac{M_{pm}}{M_p}) - 2\frac{A_f d_f}{A_w d_w}\}^2 \right] = 0$$

For

$$\frac{A_f}{A_w} = 2.0, \quad \frac{d_f}{d_w} = 1.05$$

$$\frac{\ell}{d_w} = \frac{3.185 \cdot \frac{M_{pm}}{M_P}}{\sqrt{2\left(1-9\frac{T^2}{T_y^2}\right)-27\left(\frac{M_{pm}}{M_P}-0.808\right)^2}\sqrt{1-\sqrt{1-4\frac{\left(1-9\frac{T^2}{T_y^2}\right)-27\left(\frac{M_{pm}}{M_P}-0.808\right)^2}{\left\{2\left(1-9\frac{T^2}{T_y^2}\right)-27\left(\frac{M_{pm}}{M_P}-0.808\right)^2\right\}^2}}}} \tag{22}$$

provided

$$\frac{M_{pm}}{M_p} \geqq 0.808$$

Equation (22) gives the interaction curves between $\frac{M_{pm}}{M_p}$, $\frac{T}{T_y}$ and $\frac{\ell}{d_w}$ for the case in which the neutral axis is located in the web, that is $\frac{M_{pm}}{M_p} > 0.808$, assuming $\frac{A_f}{A_w} = 2.0$ and $\frac{d_f}{d_w} = 1.05$. For the case of $\frac{M_{pm}}{M_p} \leqq 0.808$ or the neutral axis lies within the flange, the stress distribution is assumed as shown in Fig. 14 (b).

Then

$$T = \sigma_y (\eta A_f + \xi A_w)$$

where:

$$\xi = \sqrt{1 - \left(\frac{V}{V_y}\right)^2}$$

ηt = distance of penetration of yielding (Fig. 14 (b)).

From Mises' yield condition:

$$\eta = \frac{A_w}{A_f}\left[\left(1+\frac{A_f}{A_w}\right)\cdot\frac{T}{T_y} - \sqrt{1-\left(\frac{V}{V_y}\right)^2}\right]$$

$$M_{pm} = \frac{1}{2}\sigma_y A_f d_f - \frac{1}{2}\sigma_y A_f \eta\,(d_w + \eta t)$$

and

$$\frac{V}{V_y} = \frac{3}{4}\left(\frac{d_w}{\ell}\right)^2\cdot\left(1+2\cdot\frac{A_f d_f}{A_w d_w}\right)^2\cdot\left(\frac{M_{pm}}{M_p}\right)^2$$

Therefore

$$\left(\frac{V}{V_y}\right)^4 - \left[2+\frac{2b}{w}\left(1+2\frac{A_f d_f}{A_w d_w}\right)\left(\frac{M_{pm}}{M_p}\right) - \frac{4b}{w}\left(1+\frac{A_f}{A_w}\right)\left(\frac{T}{T_y}\right) - 2\left(1+\frac{A_f}{A_w}\right)^2\left(\frac{T}{T_y}\right)^2 - \frac{4b}{w}\cdot\frac{A_f d_f}{A_w d_w} - \frac{4b^2}{w^2}\right]\cdot\left(\frac{V}{V_y}\right)^2$$

$$+\left[\frac{b}{w}\left(1+2\frac{A_f d_f}{A_w d_w}\right)\left(\frac{M_{pm}}{M_p}\right) + \frac{2b}{w}\left(1+\frac{A_f}{A_w}\right)\left(\frac{T}{T_y}\right) + \left(1+\frac{A_f}{A_w}\right)^2\left(\frac{T}{T_y}\right)^2 - \frac{2b}{w}\cdot\frac{A_f d_f}{A_w d_w} + 1\right]^2$$

$$-\left[\frac{2b}{w} + 2\left(1+\frac{A_f}{A_w}\right)\left(\frac{T}{T_y}\right)\right]^2 = 0$$

For

$$\frac{A_f}{A_w} = 2.0, \quad \frac{d_f}{d_w} = 1.05,$$

$$\frac{V}{V_y} = \sqrt{\left[883 + 120\left(\frac{T}{T_y}\right) + 9\left(\frac{T}{T_y}\right)^2 - 104\left(\frac{M_{pm}}{M_p}\right)\right]\left[\sqrt{1 + \frac{\left\{40 + 6\left(\frac{T}{T_y}\right)\right\}^2 - \left\{104\left(\frac{M_{pm}}{M_p}\right) + 120\left(\frac{T}{T_y}\right) + 9\left(\frac{T}{T_y}\right)^2 - 83\right\}^2}{\left\{883 + 120\left(\frac{T}{T_y}\right) + 9\left(\frac{T}{T_y}\right)^2 - 104\left(\frac{M_{pm}}{M_p}\right)\right\}^2}} - 1\right]}$$

or

$$\frac{\ell}{d_w} = \frac{4.50\left(\frac{M_{pm}}{M_p}\right)}{\sqrt{\left\{883 + 120\left(\frac{T}{T_y}\right) + 9\left(\frac{T}{T_y}\right)^2 - 104\left(\frac{M_{pm}}{M_p}\right)\right\}\left[\sqrt{1 + \frac{\left\{40 + 6\left(\frac{T}{T_y}\right)\right\}^2 - \left\{104\left(\frac{M_{pm}}{M_p}\right) + 120\left(\frac{T}{T_y}\right) + 9\left(\frac{T}{T_y}\right)^2 - 83\right\}^2}{\left\{883 + 120\left(\frac{T}{T_y}\right) + 9\left(\frac{T}{T_y}\right)^2 - 104\left(\frac{M_{pm}}{M_p}\right)\right\}^2}} - 1\right]}} \tag{23}$$

provided

$$\frac{M_{pm}}{M_p} \leqq 0.808 \quad \text{for} \quad \frac{A_f}{A_w} = 2.0 \quad \text{and} \quad \frac{d_f}{d_w} = 1.05$$

Equations (22) and (23) are connected together at $\frac{M_{pm}}{M_p} = 0.808$ as shown in Fig. 14. Figure 14 shows that the reduction in the plastic moment due to shear becomes less for higher values of the axial force. In other words, it is not necessary to consider the effect of shear if a high axial force is present.

The reduction in the plastic moment is due mainly to the influence of this axial force. Figure 15 shows the reduction of the plastic moment for a constant ratio of length to depth of a cantilever beam, $\ell/d_w = 2.0$, due to various values of axial force. The two curves shown are cross curves of Fig. 13 and 14 at $\ell/d_w = 2.0$. The test points obtained from experiments reported in the first part of this paper are also plotted. They show a surprisingly fair correlation with approach (B) rather than approach (A). This means that the assumed stress distribution of approach (B) leads to results which are satisfactory for design purposes.

4.2 Deflection of Beams in Strain-Hardening Range

a) Assumptions(13)

The actual moment curvature relation for a wide flange section is approximated by an idealized curve as shown in Fig. 17 (a). This curve consists of a straight line from an elastic limit at $M/M_{pm} = 0.915$ to the line $M/M_{pm} = 1$ at $\phi/\phi_{pm} = 2.0$. The latter selection of the point where the cross-section is considered to be fully yielded is quite arbitrary. The extent of yielding in the flange is then given by

$$\alpha = 1 - 0.915 \frac{M_{pm}}{M_o}$$

b) Equivalent Hinge Rotation

From Fig. 17 (b) the inelastic angular rotation θ can be computed by integrating the inelastic part of the curvature

diagram. It consists of three parts: The first part (designated as (1) in Fig. 17 (b)) is the region between M_{pm} and M_o. For the time being it is assumed that the slope of the moment vs. curvature curve in the strain-hardening region is the same as in the elastic region. A correction of this assumption will be introduced as part two. Hence:

$$\theta_1 = \bar{z}(\phi_{st} - \phi_{pm})$$

where

$$\phi_{pm} = \frac{M_{pm}}{EI}$$

$$\bar{z} = \frac{M_o - M_{pm}}{M_o} \cdot \ell$$

Therefore

$$\frac{\theta_1}{\ell \phi_{pm}} = \left(\frac{\phi_{st}}{\phi_{pm}} - 1\right)\left(1 - \frac{M_{pm}}{M_o}\right) \qquad (24)$$

The second part, shown as (2) in Fig. 17 (b) comes from the difference between the bending stiffness in the strain-hardening region, $E_{sh} \cdot I$, and that in the elastic region, EI.

Therefore

$$\theta_2 = \frac{\bar{z}}{2}\left[(M_o - M_{pm})\left(\frac{1}{E_{st} I} - \frac{1}{EI}\right)\right]$$

or

$$\frac{\theta_2}{\ell \phi_{pm}} = \frac{1}{2}\left(\frac{M_o}{M_{pm}} - 1\right)\left(\frac{E}{E_{st}} - 1\right)\left(1 - \frac{M_{pm}}{M_o}\right) \qquad (25)$$

The third part is the region (3) in Fig. 17 (b) due essentially to the progressive plastification of the cross-section. Its extent depends also on the residual stress in rolled sections.

$$\theta_3 = \frac{1}{2}\,\bar{\bar{z}}\cdot\phi_{pm}$$

where

$$\bar{z} + \bar{\bar{z}} = \left(1 - 0{,}915\,\frac{M_{pm}}{M_o}\right)\cdot \ell$$

or

$$\bar{\bar{z}} = 0{,}085\cdot\frac{M_{pm}}{M_o}\cdot \ell$$

Therefore

$$\frac{\theta_3}{\ell\,\phi_{pm}} = 0{,}0425\,\frac{M_{pm}}{M_o} \qquad (26)$$

Adding Eq. (24), (25) and (26), the total inelastic angle is

$$\frac{\theta}{\ell\,\phi_{pm}} = \left[\left(\frac{\phi_{st}}{\phi_{pm}} - 1\right) + \frac{1}{2}\left(\frac{M_o}{M_{pm}} - 1\right)\left(\frac{E}{E_{st}} - 1\right)\right]\left(1 - \frac{M_{pm}}{M_o}\right) + 0{,}0425\,\frac{M_{pm}}{M_o}$$

where

$$\frac{\phi_{st}}{\phi_{pm}} = \frac{\phi_{st}}{\phi_p}\cdot\frac{M_p}{M_{pm}} = \frac{\phi_{st}}{K\,\phi_p}$$

$$\frac{M_o}{M_{pm}} = \frac{M_o}{M_p}\cdot\frac{M_p}{M_{pm}} = \frac{M_o}{K\,M_p}$$

and K = reduction factor of M_p due to shear and thrust = $\frac{M_{pm}}{M_p}$.

For structural steels, ASTM-A7[14]

$$E = 30{,}000 \text{ ksi}$$

$$E_{st} = 900 \text{ ksi}$$

$$\phi_{sh} = 12\,\phi_p$$

Therefore

$$\frac{\theta}{l\phi_p} = \left[(12-K) + \frac{97}{6}\left(\frac{M_o}{M_p} - K\right)\right]\left(1 - \frac{KM_p}{M_o}\right) + 0.0425\,K^2\frac{M_p}{M_o} \quad (27)$$

where $M_o = Vl$, V = shear force

c) Computation of Deflection

Deflection of the beam in strain-hardening range may be constructed by the following components.

1. Elastic deflection due to bending up to elastic limit shear V_u.
2. Elastic deflection due to shear up to elastic limit shear V_u.
3. Deflection due to hinge rotation.
4. Deflection due to bending in strain-hardening region for ΔV, where $\Delta V = V - V_u$.
5. Deflection due to shear in strain-hardening region for ΔV.

The total deflection is given by

$$\delta = \delta_1 + \delta_2 + \delta_3 + \delta_4 + \delta_5 \quad (28)$$

where

$$\delta_1 = \frac{V_u(2\ell^3 - 3\ell^2 x + x^3)}{6EI} \quad ; \; x = \text{distance from free end}$$

$$\delta_2 = \frac{V_u(\ell - x)}{GA_w}$$

$$\delta_3 = (\ell - x)\cdot\theta \quad ; \; \theta \text{ is given by Eq. (27)}$$

$$\delta_4 = \frac{\Delta V(2\ell^3 - 3\ell^2 x + x^3)}{6E_{st}I}$$

$$\delta_5 = \frac{\Delta V(\ell - x)}{G_{st}A_w}$$

G_{st} = shear modulus in strain-hardening range = 2,400 ksi (14)

The deflection for each specimen No. 1, 2 and 3 were computed in this fashion and are plotted in Fig. 3 in dashed lines. These curves for the deflections of the beam in strain-hardening range show fair correlation with the test results as may be seen in Fig. 3.

V. APPLICATION OF RESULTS TO DESIGN PROBLEM —ULTIMATE LOAD OF BEAM WITH CUT-OUT—

A simply supported beam with a cut-out is subjected to a transverse concentrated load at an arbitrary position as shown in Fig. 18 (a). Although the beam is externally statically determinate it is internally three times statically indeterminate as can be readily seen. Using "Plastic Analysis" the numbers of possible hinges are five, four around the cut-out and one under the concentrated load. Subtracting the number of redundants from the number of possible hinges furnishes the number of independent mechanisms. These two mechanisms are illustrated in Fig. 18 (b) and (c).

Let M_p be the full plastic moment of the beam at the cut-out and mM_p be that of the original beam. Neglecting for the time being any influence of shear and axial force, the ultimate load corresponding to mechanism (I) in Fig. 18 (b) is given by

$$P_I = \frac{2L}{\ell - \ell_4} \cdot M_p$$

and for mechanism (II) in Fig. 18 (c) by

$$P_{II} = \frac{L}{\ell_3 \ell_4} \cdot mM_p$$

Comparing these two loads it is concluded that mechanism (I) will occur when

$$m > 2\,\frac{\ell_3}{\ell}$$

In most built-up beams with cut-out, however, the influence of high thrust and shear forces at the cut-out causes a considerable reduction in the plastic moment. Cross-sections through the beam at A-A and B-B are shown in Fig. 18 (d). For mechanism (I) the condition of forces in Fig. 18 (b) is given by the following equations.

$$V_u = V_L = \frac{1}{2} V \quad \text{for} \quad d_1 = d_2$$

$$M_u = M_L = M_{pm} = \frac{1}{2} V \ell$$

where M_{pm} = reduced plastic moment due to shear and thrust

The equilibrium equation is

$$V \frac{\ell}{2} = M_u + M_L + Th$$

and $$V = \frac{\ell_4}{L} P_u$$

where P_u = ultimate load

Therefore $$T = \frac{\ell_2 - \ell}{h} \cdot \frac{\ell_4}{L} \cdot P_u = \frac{\ell'}{h} \cdot \frac{\ell_4}{L} \cdot P_u$$

or $$T = 2 \frac{\ell'}{h} \cdot \frac{M_{pm}}{\ell} \qquad (29)$$

$$P_u = 2 \frac{L}{\ell_4} \cdot \frac{M_{pm}}{\ell} \qquad (30)$$

From the interaction curves of M, T and V in Fig. 14 which are computed by using the approach (B) and from the Eq. (29), the reduced plastic moment M_{pm} can be obtained by means of an iteration method. Then the ultimate load P_u is given by

Eq. (30). For example, taking $d = \frac{L}{6}$, $h' = \frac{L}{8}$ and $\ell' = \frac{L}{3}$, the ultimate load is computed as a function of the length of the cut-out in the following manner.

$$\frac{A_f}{A_w} = 2.0 \text{ and } \frac{d_f}{d_w} = 1.05$$

Therefore

$$\frac{\ell}{L} = 0.040 \quad 0.045 \quad 0.050 \quad 0.075 \quad 0.100$$

$$\frac{\ell}{d_w} = 2.112 \quad 2.376 \quad 2.640 \quad 3.960 \quad 5.280$$

For $\frac{\ell}{d_w} = 2.112$ ($\frac{\ell}{L} = 0.04$), assume $\frac{T}{T_y} = 0.60$ as a first approximation, then from Fig. 14

$$\frac{M_{pm}}{M_p} = 0.445$$

Therefore from Eq. (29),

$$\frac{T}{T_y} = 0.42$$

Repeating this process as follows,

T/T_y = 0.60 ↓ 0.42 ↑ 0.57 ↓ 0.45 ↑ 0.54 ↓ 0.47 ↑ 0.52 ↓ 0.49 ↑ 0.50 ↓ 0.50

M_{pm}/M_p = 0.445 0.605 0.475 0.58 0.50 0.56 0.52 0.53 0.53 0.53

this iteration method converges to

$$T/T_y = 0.50$$

$$M_{pm}/M_p = 0.53$$

Therefore

$$\frac{\ell 4}{L} \cdot \frac{P_u}{\sigma_y A_o} = 0.0616$$

where A_o is the total cross-sectional area at section B-B in Fig. 18 (d). In a similar way the following values are obtained by the iteration method.

ℓ/L =	0.01	0.02	0.025	0.035	0.04	0.075	0.100
ℓ/d_w =	0.528	1.056	1.320	1.850	2.112	3.960	5.280
M_{pm}/M_p =	0.230	0.465	0.390	0.495	0.530	0.735	0.815
$\frac{\ell 4}{L} \cdot \frac{P_u}{\sigma_y A_o}$ =	0.106	0.106	0.0718	0.0650	0.0616	0.0450	0.0375

These results are shown in Fig. 18 (e). For this example, both beams at the cut-out may fail by shear if the ratio of length of the cut-out over length of the beam is less than 0.04. In the region the ultimate load P_u is independent of the length of the cut-out.

For the case in which the ratio is greater than 0.04 the beam fails in the fashion of bending type at the reduced plastic moment M_{pm} under the influence of shear and axial forces.

VI. SUMMARY OF RESULTS AND CONCLUSIONS

The influence of both shear and axial forces on the plastic moment of a wide flange cantilever beam was studied theoretically on the basis of a lower bound method of plastic analysis. Two

approaches were proposed, the difference being in the derivation of the shearing stress. Both approaches give good correlations with test results for a small axial force. However, one of the two methods is valid even under high axial force. The confirming tests show that this approach (B), based on the average shearing stress method gives fair prediction even for a relatively short beam ($\ell/d_w = 2.0$) under the combination of high axial and shear forces (Fig. 15). The interaction curves between moment, shear and axial forces based on approach (B) were computed for the case of $\frac{A_f}{d_w} = 2.0$ and $\frac{d_f}{d_w} = 1.05$ which are representative values for most wide flange beams. As can be seen from Fig. 14, the reduction of the plastic moment is mainly due to axial force when $\ell/d_w \geq 5.0$.

The question arises if the influence of shear and axial force on the plastic moment cannot be obtained by investigating the two effects separately and superimposing the two reductions. If the T/T_y ratio is not too high and also if the ℓ/d_w ratio is not too small, then the reduction of the plastic moment as illustrated in Fig. 14 is very close to the reduction obtained by superposition of these two effects. In other words, the following simplified approach can be used

$$\frac{M_{pm}}{M_p} \cong \frac{M_{ps}}{M_p} \times \frac{M_{pc}}{M_p} \tag{31}$$

where

M_p = full plastic moment of the cross-section

M_{pm} = reduced plastic moment due to shear and thrust

M_{ps} = reduced plastic moment due to shear only

M_{pc} = reduced plastic moment due to thrust only

and also

$$\frac{M_{ps}}{M_p} = \frac{8}{9} \cdot \frac{t\ell^2}{Z}\left[\sqrt{1 + \frac{9}{4} \cdot \frac{Z}{t\ell^2}} - 1\right] \qquad (32)$$

$$\frac{M_{pc}}{M_p} = 1 - \frac{A^2}{4tZ} \cdot \left(\frac{T}{T_y}\right) \text{ (neutral axis in web)} \qquad (33)$$

$$= \frac{A}{2Z}\left(1 - \frac{T}{T_y}\right) \cdot \left[d - \frac{A}{2b}\left(1 - \frac{T}{T_y}\right)\right] \text{ (neutral axis in flange)}$$

Equation (31) can also be expressed as

$$\left(1 - \frac{M_{pm}}{M_p}\right) \cong \left(1 - \frac{M_{ps}}{M_p}\right) + \left(1 - \frac{M_{pc}}{M_p}\right) \qquad (34)$$

This means that the reduction of the plastic moment in percent due to the combination of shear and axial forces is equal to the sum of reduction in percent due to shear and axial force respectively. For design purposes, Eq. (34) with Eq. (32) and (33) is simple and also practical. The error of this approximation is within 3% compared to the approach (B) over a considerable range of ℓ/d_w and T/T_y.

The deflection of a beam in the strain-hardening range can be predicted with fair accuracy as shown by the test results illustrated in Fig. 3. In the analysis the deflection was

separated into the following three components:

1. Elastic deflection due to bending and shear up to elastic limit shear V_u, corresponding to the theoretical failure load P_u.
2. Deflection due to hinge rotation given by Eq. (27).
3. Deflection due to bending and shear in the strain-hardening range for ΔV where $\Delta V = V - V_u$.

Finally the theoretical failure load P_u for a built-up beam with cut-out was computed by means of iteration method using the iteraction curves of M, V and T in Fig. 14. The result is given in Fig. 18 (e) showing the range of shear failure and bending failure respectively.

VII. ACKNOWLEDGEMENTS

This work has been carried out at the Fritz Engineering Laboratory, Lehigh University, Bethlehem, Pennsylvania, as a partial study of the project "Built-Up Members in Plastic Design", sponsored by the Welding Research Council and the Department of the Navy, with funds provided by the American Institute of Steel Construction, the American Iron and Steel Institute, the Office of Naval Research, the Bureau of Ships and the Bureau of Yards and Docks. The project is under the general direction of Dr. Lynn S. Beedle. Professor William J. Eney is Director of Fritz Engineering Laboratory and Head of the Department of Civil Engineering.

The authors wish to acknowledge the helpful suggestions given by staff members of Lehigh Project Subcommittee, of which Mr. T. R. Higgins is chairman. The assistance furnished by members of the Fritz Engineering Laboratory staff in the preparation of the test specimens is gratefully acknowledged.

VIII. REFERENCES

1. Horne, M. R. — THE PLASTIC THEORY OF BENDING OF MILD STEEL BEAMS WITH PARTICULAR REFERENCE TO THE EFFECT OF SHEAR FORCES Proceedings of the Royal Society of London, Series A, Vol. 207, 1951

2. Fujita, Y. — INFLUENCE OF SHEAR ON THE FULL PLASTIC MOMENT OF BEAMS C.E. 404 Report, Lehigh University 1955

3. Beedle, L. S. Thürlimann, B. Ketter, R. L. — PLASTIC DESIGN IN STRUCTURAL STEEL Lehigh University - American Institute of Steel Construction, Summer Course 1955

4. Green, A. P. — A THEORY OF THE PLASTIC YIELDING DUE TO BENDING OF CANTILEVERS AND FIXED-ENDED BEAMS Journal of Mechanics and Physics of Solids, Vol. 3, 1954

5. Leth, C. F. — THE EFFECT OF SHEAR STRESSES ON THE CARRYING CAPACITY OF I-BEAM Brown University Technical Report 107 to Office of Naval Research, Contract No. 7 ONR - 35801, March 1954

6. Shield, R. T. — THE INFLUENCE OF SHEARING FORCES ON THE PLASTIC BENDING OF WIDE BEAMS Proceedings of the Second U. S. National Congress of Applied Mechanics, June 1954

7. Drucker, D. C. — THE EFFECT OF SHEAR ON THE PLASTIC BENDING OF BEAMS Brown University Technical Report 56-APM-28 to Office of Naval Research, Contract No. DA-19-020-ORD-3172 December 1955

8. Ketter, R. L. Beedle, L. S. Johnston, B. G. — COLUMN STRENGTH UNDER COMBINED BENDING AND THRUST The Welding Journal, 31 (12) Research Supplement, 1952

9. Onat, E. T. Prager, W. — THE INFLUENCE OF AXIAL FORCES ON THE COLLAPSE LOAD OF FRAMES Proceedings of the First Midwest Conference on Solid Mechanics, 1953

10. Horne, M. R. — THE FULL PLASTIC MOMENTS OF SECTIONS SUBJECTED TO SHEAR FORCE AND AXIAL LOAD British Welding Journal, April 1958

11. Prager, W.
Hodge, P. G.
THEORY OF PERFECTLY PLASTIC SOLIDS
John Wiley, New York 1951

12. Heyman, J.
Dutton, V. L.
PLASTIC DESIGN OF PLATE GIRDERS WITH UNSTIFFENED WEBS
Welding and Metal Fabrication, 22, 265 (1954)

13. White, M. W.
THE LATERAL-TORSIONAL BUCKLING OF YIELDED STRUCTURAL STEEL MEMBERS
Welded Continuous Frames and Their Components, Interim Report No. 32, Institute of Research, Lehigh University, October 1956

14. Haaijer, G.
Thurlimann, B.
ON INELASTIC BUCKLING IN STEEL
Proceedings of the American Society of Civil Engineers, Vol. 84, No. EM2, April 1958

IX. NOMENCLATURE

A = total cross-sectional area of wide flange shapes

A_o = cross-sectional area of built-up beam at section B-B in Fig. 18 (a)

A_f = total flange area of wide flange shapes

A_w = web area of wide flange shapes

α = coefficient of extent of strain-hardening region

b = flange width

d = depth of wide flange shapes

d_f = distance between center line of flanges

d_w = depth of web

$\delta, \delta_1, \delta_2, \delta_3, \delta_4, \delta_5$ = deflections

δ_{RP} = readings of a dial gage for rotation measurement

Δ = deflection of a beam at a reference point of the rotation gage

E = Young's modulus

E_{st} = strain-hardening modulus

G = shear modulus

G_{st} = shear modulus in strain-hardening region

I = moment of inertia of a cross-section

K = reduction factor in full plastic moment due to shear and axial forces

L = length of built-up beam

ℓ = length of a cantilever beam

M_p = full plastic moment of cross-section

M_{pc} = reduced plastic moment due to axial force

M_o = fixed end moment of a cantilever beam

M_{pm} = reduced plastic moment due to shear and axial forces

M_{ps} = reduced plastic moment due to shear force

P_u = theoretical ultimate load or "failure" load of wide flange shapes

ϕ_{pm} = curvature corresponding to M_{pm}

ϕ_{st} = curvature at the starting point of strain-hardening

r_{yy} = radius of gyration of wide flange shapes about weak axis

S = section modulus of cross-section

σ_y = static yield stress

θ_e = corresponding angle rotation resulted from deflection due to shear in elastic region

θ_p = hinge rotation angle

t = thickness of flange plate

T = axial force

T_y = axial yield force = $\sigma_y A$

τ = shearing stress

V = shear force

V_u = shear force at P_u

V_y = shear yield force = $\tau_y A_w$

ΔV = $V - V_u$

x = distance from free end of a cantilever beam

y = distance from neutral axis of cross-section

Z = plastic modulus of wide flange shapes

w = thickness of web plate

X. TABLES AND FIGURES

Comparison of Theoretical "Failure"

Load P_u Obtained from Different Methods

	Methods	No. 1 $T/T_y = 0.13$	No. 2 $T/T_y = 0.19$	No. 3 $T/T_y = 0.37$
1	Deflection I (3")	70 kips	82 kips	126 kips
2	Deflection II (7")	70	82	126
3	Deflection III (11")	70	82	126
4	Curvature	70	85	126
5	Hinge Rotation	70	82	120
6	Theoretical (A)	73	82	79
7	Theoretical (B)	70	82	124

TABLE I

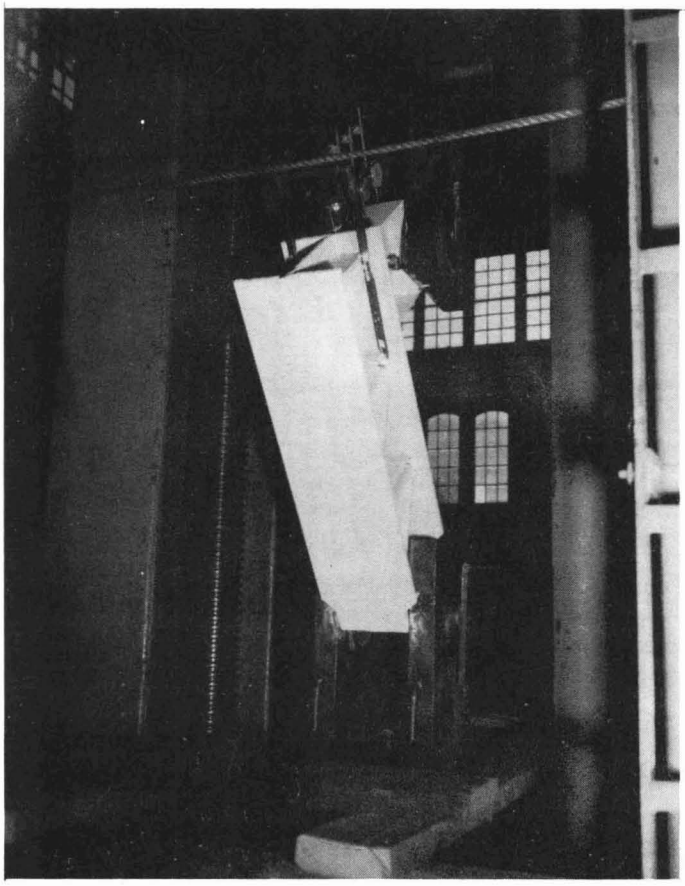

PHOTO 1 - TEST SET-UP

PHOTO 2 - TESTING MACHINE

PHOTO 3 - MODE OF FAILURE OF SPECIMENS

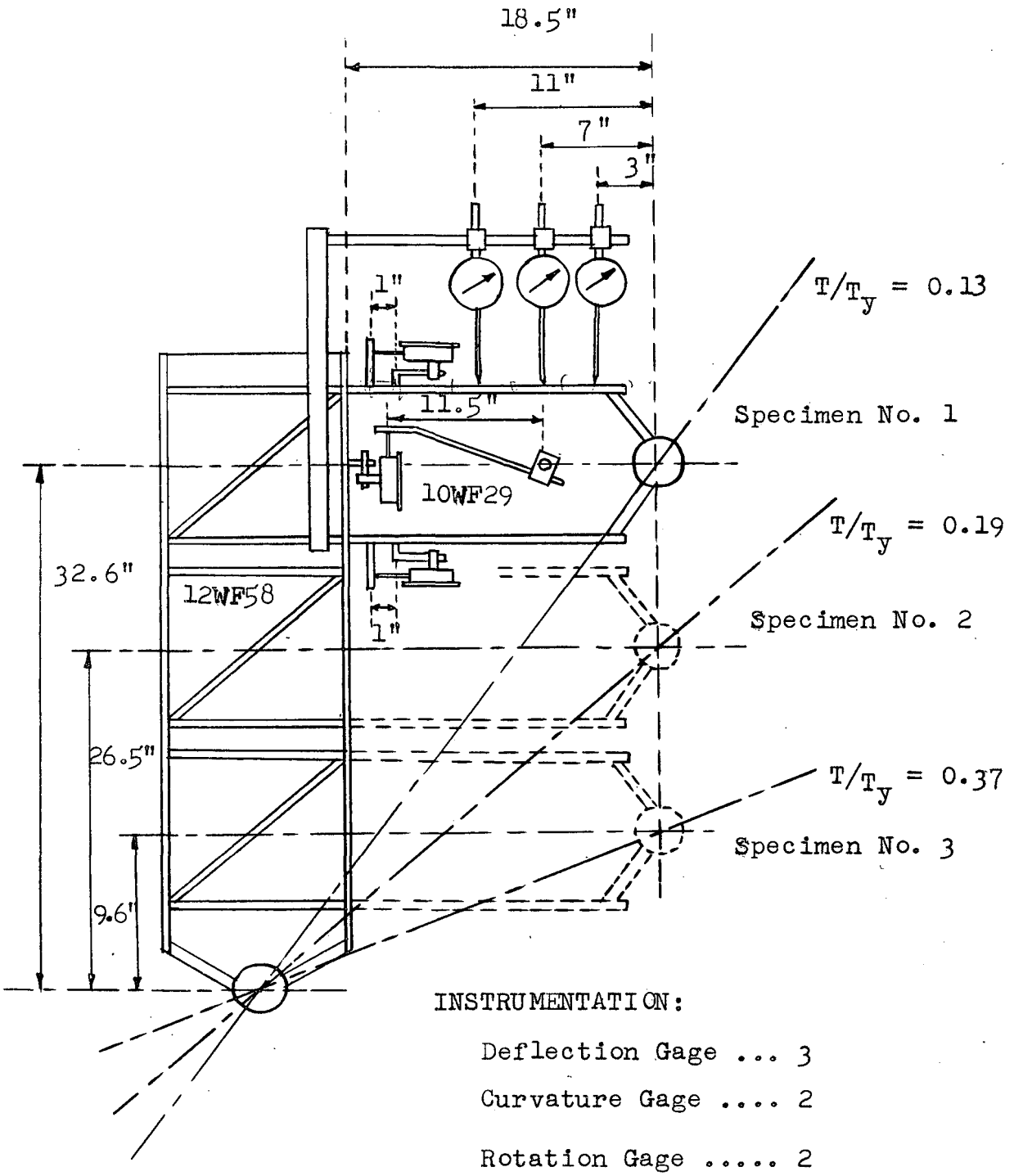

FIG. 1 - TEST SPECIMENS AND INSTRUMENTATION

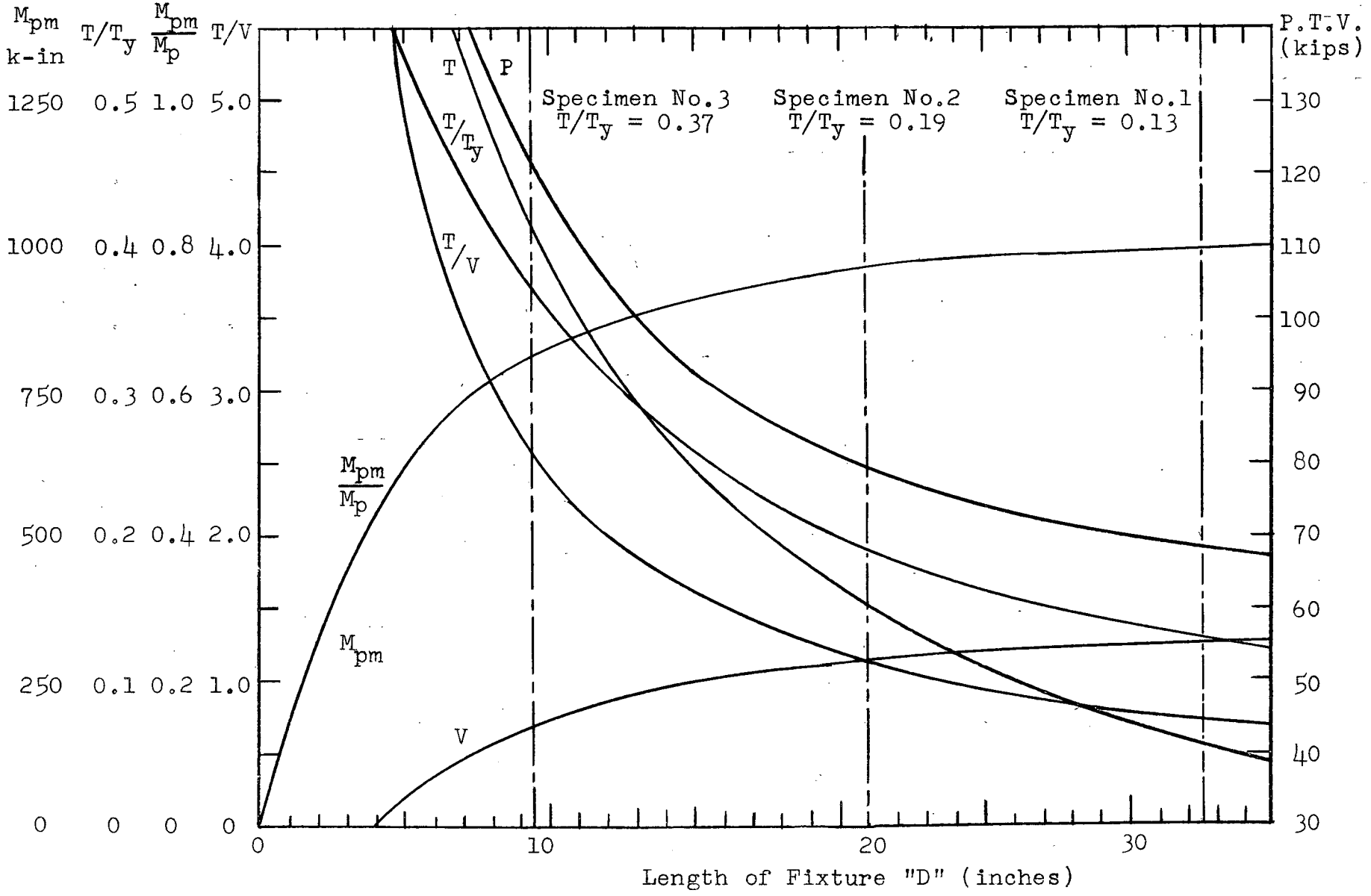

FIG. 2 - CONTROL CURVES FOR TEST SET-UP

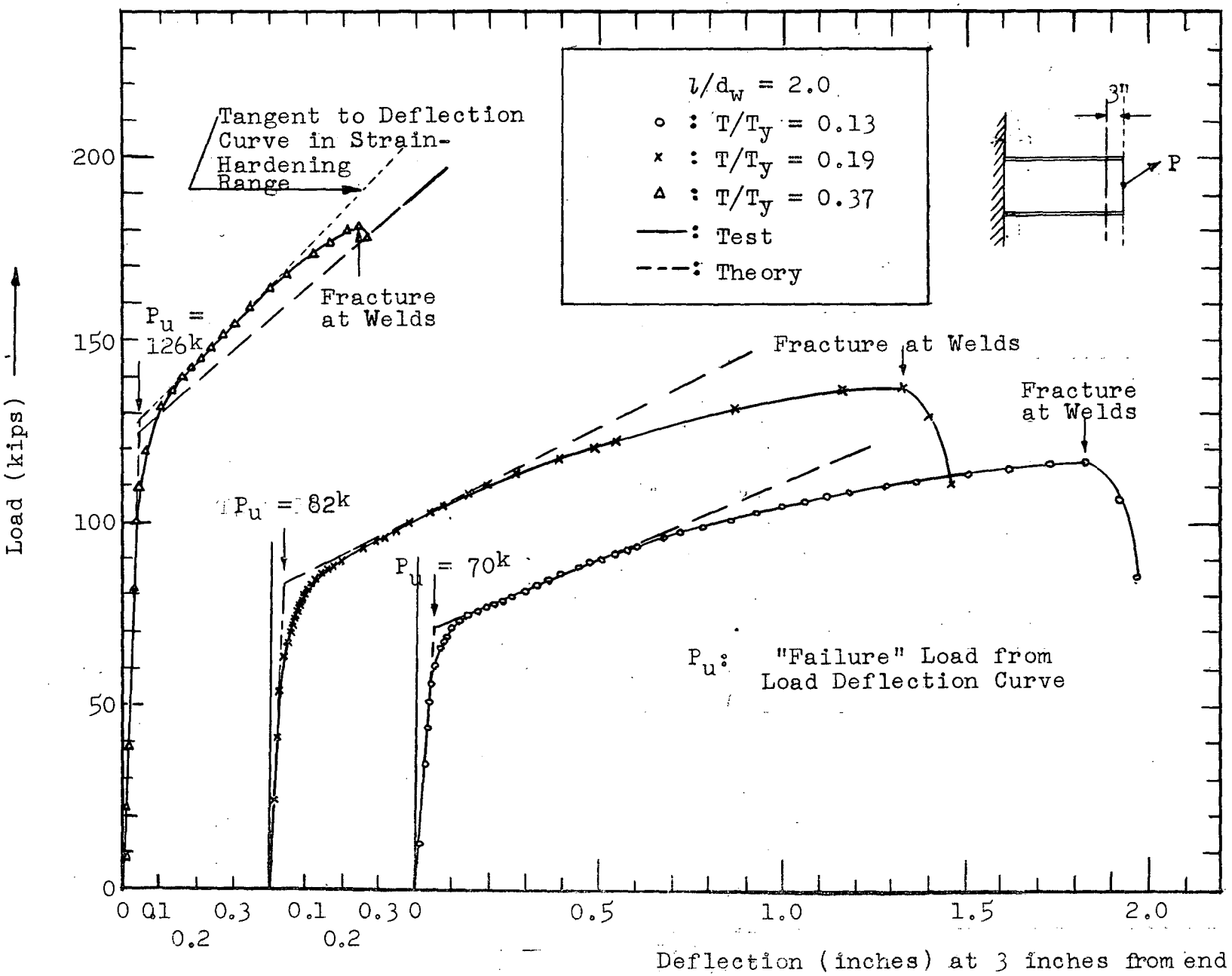

FIG. 3 - LOAD-DEFLECTION CURVES (I)

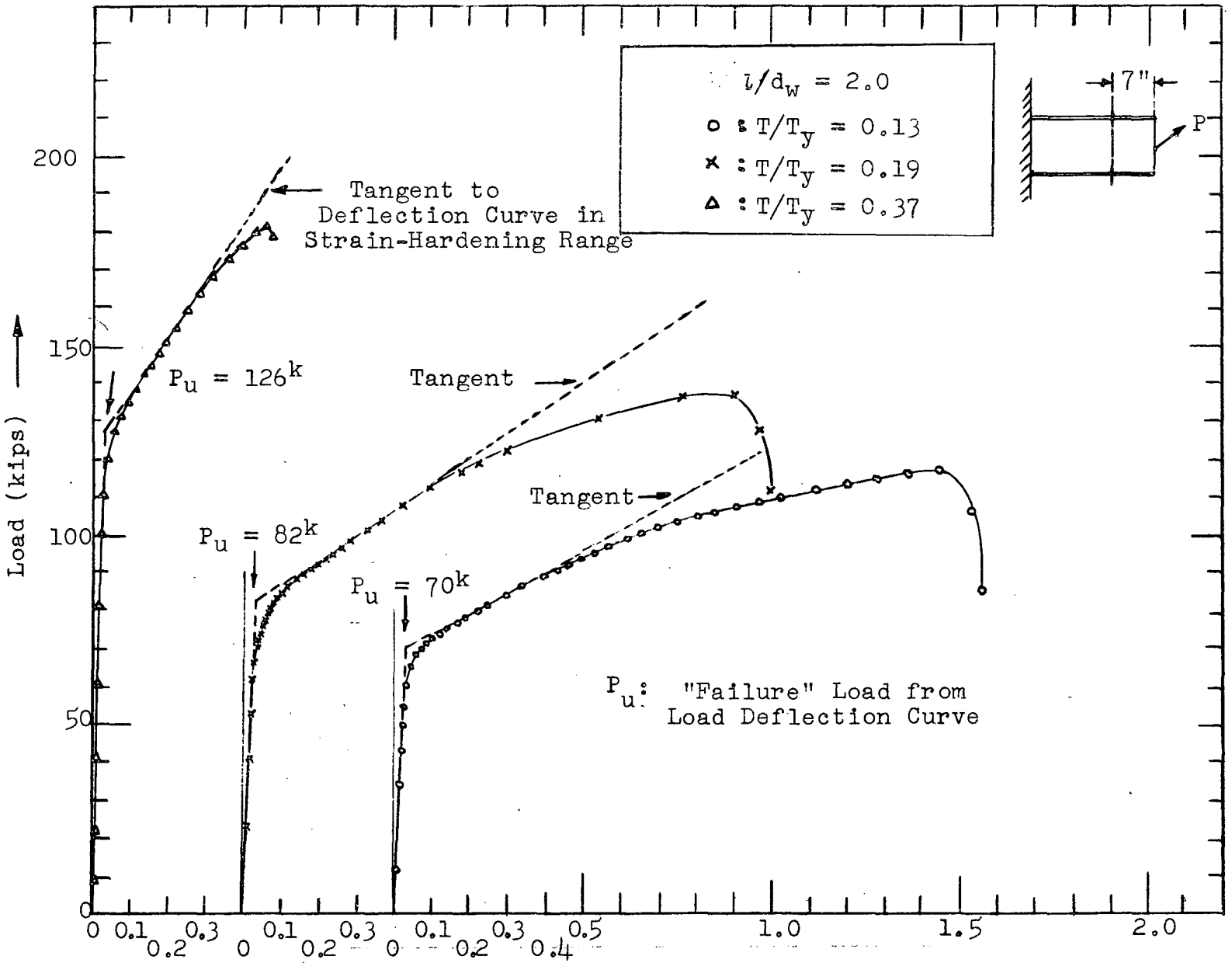

FIG. 4 - LOAD-DEFLECTION CURVES (II)

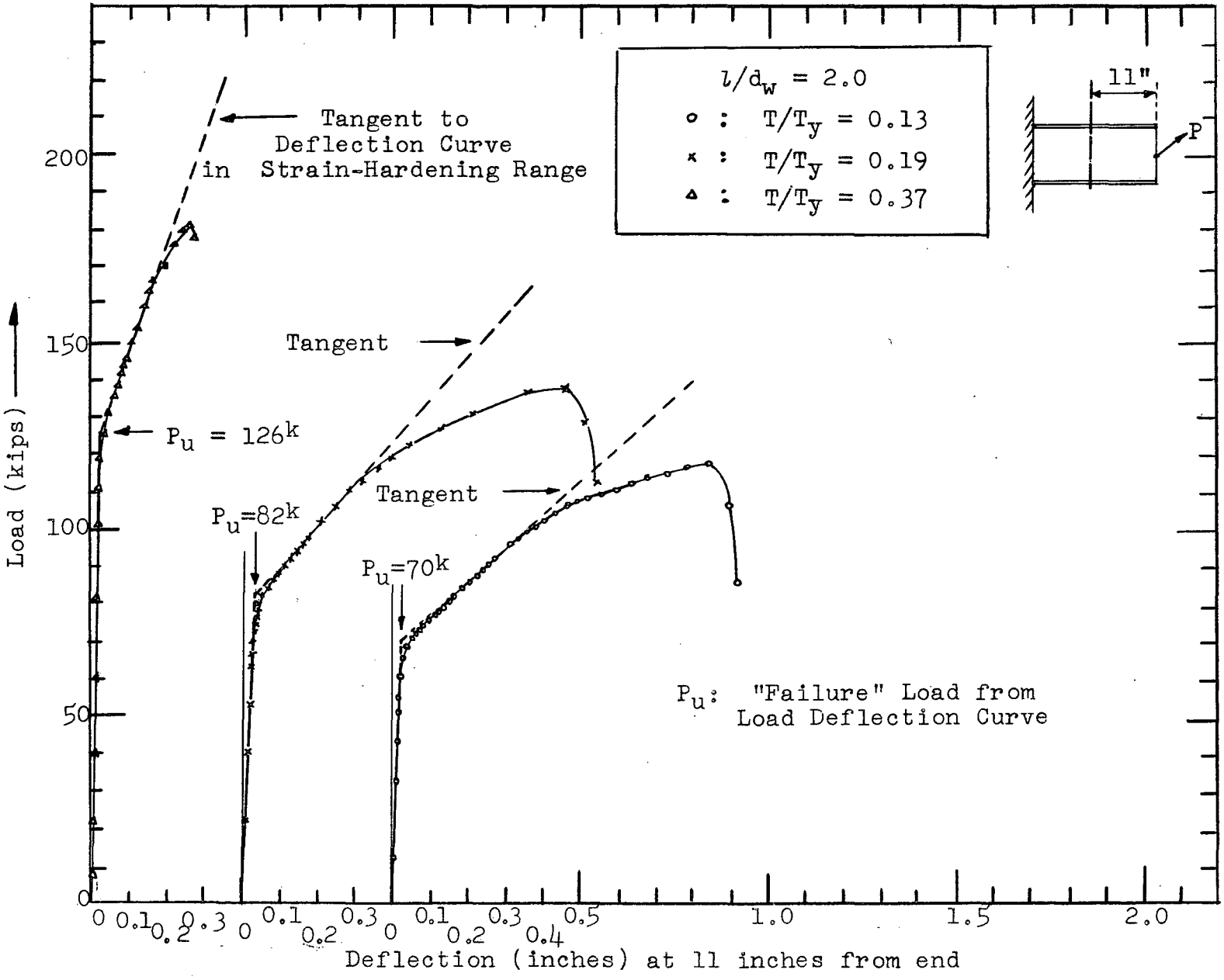

FIG. 5 - LOAD-DEFLECTION CURVES (III)

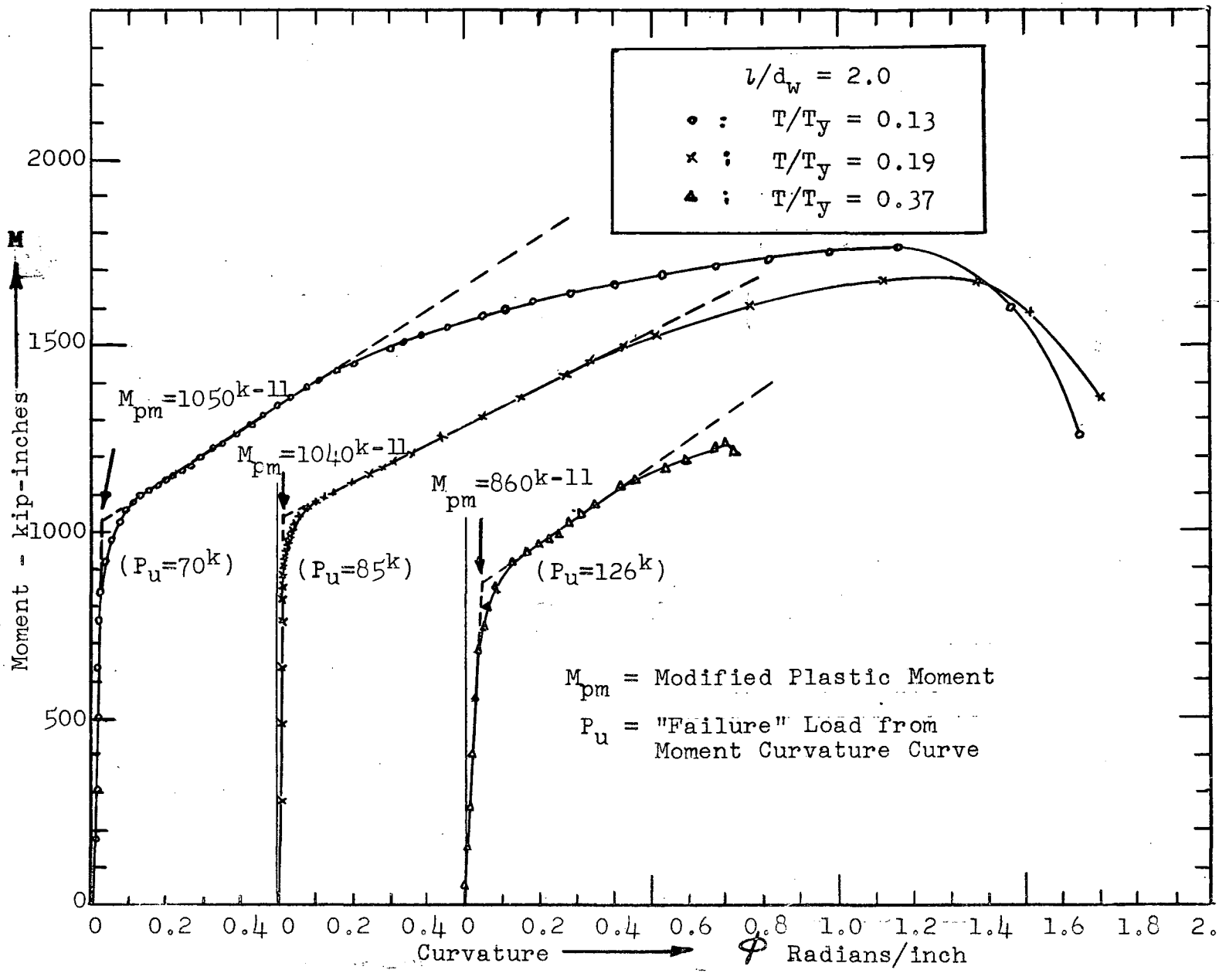

FIG. 6 - MOMENT-CURVATURE DIAGRAM

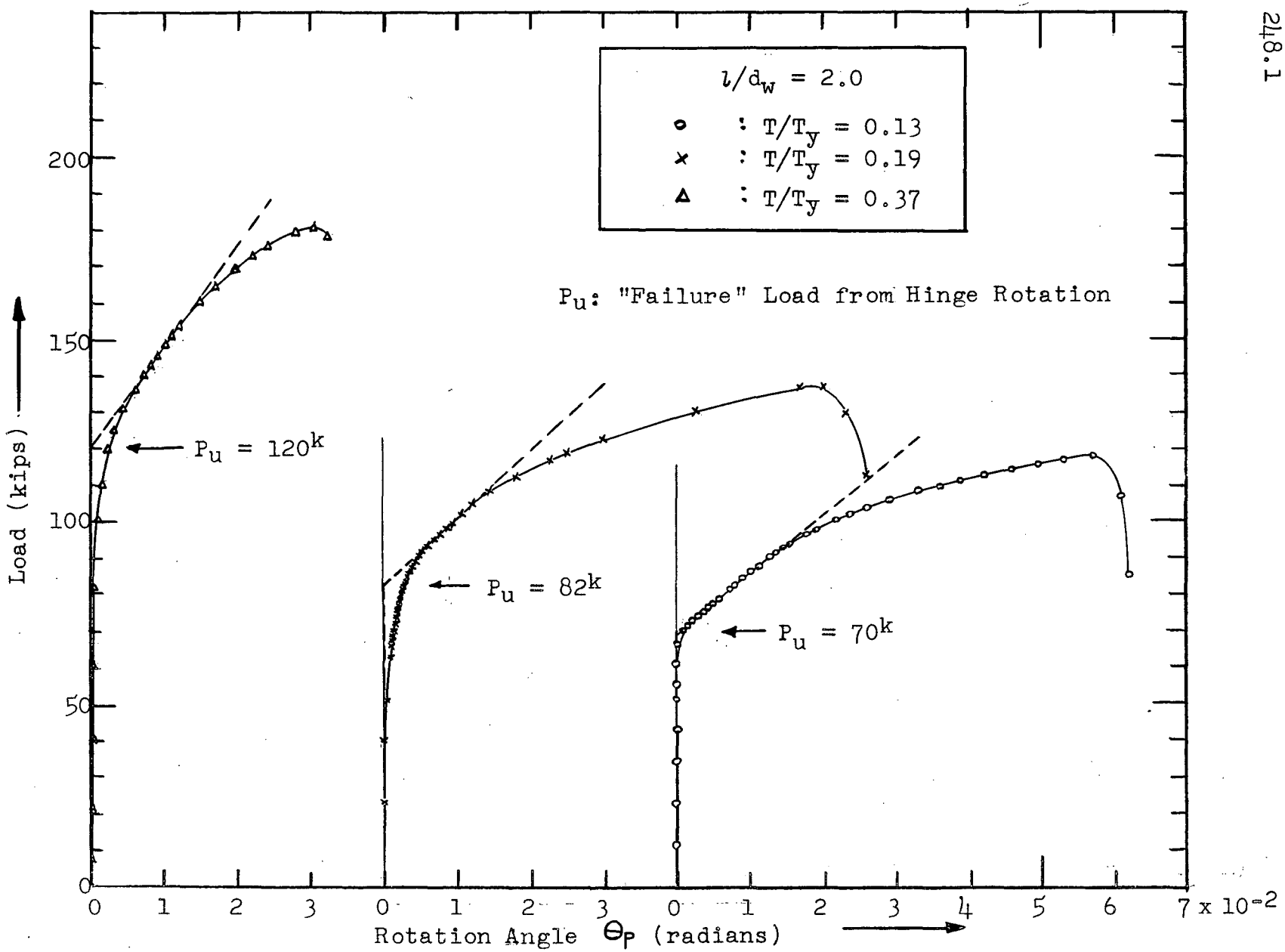

FIG. 7 - EQUIVALENT HINGE ROTATION

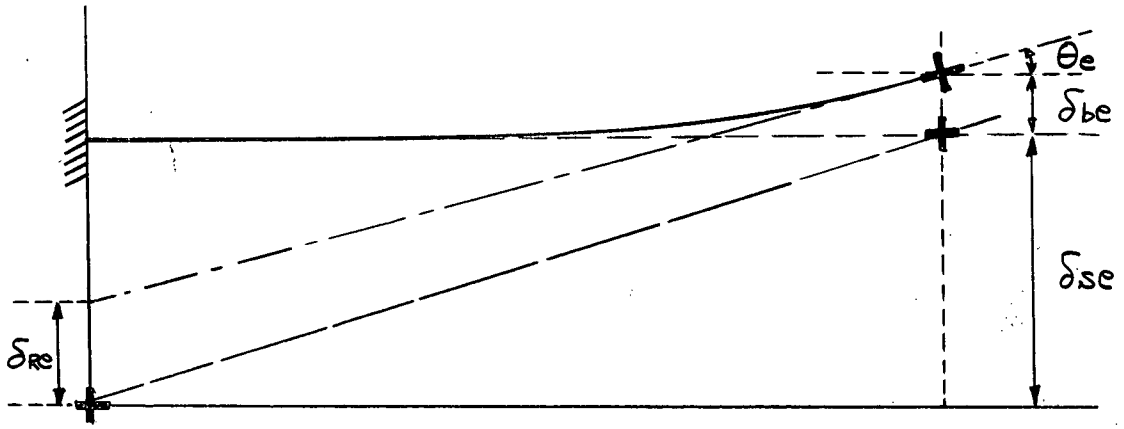

(a) Elastic Bending

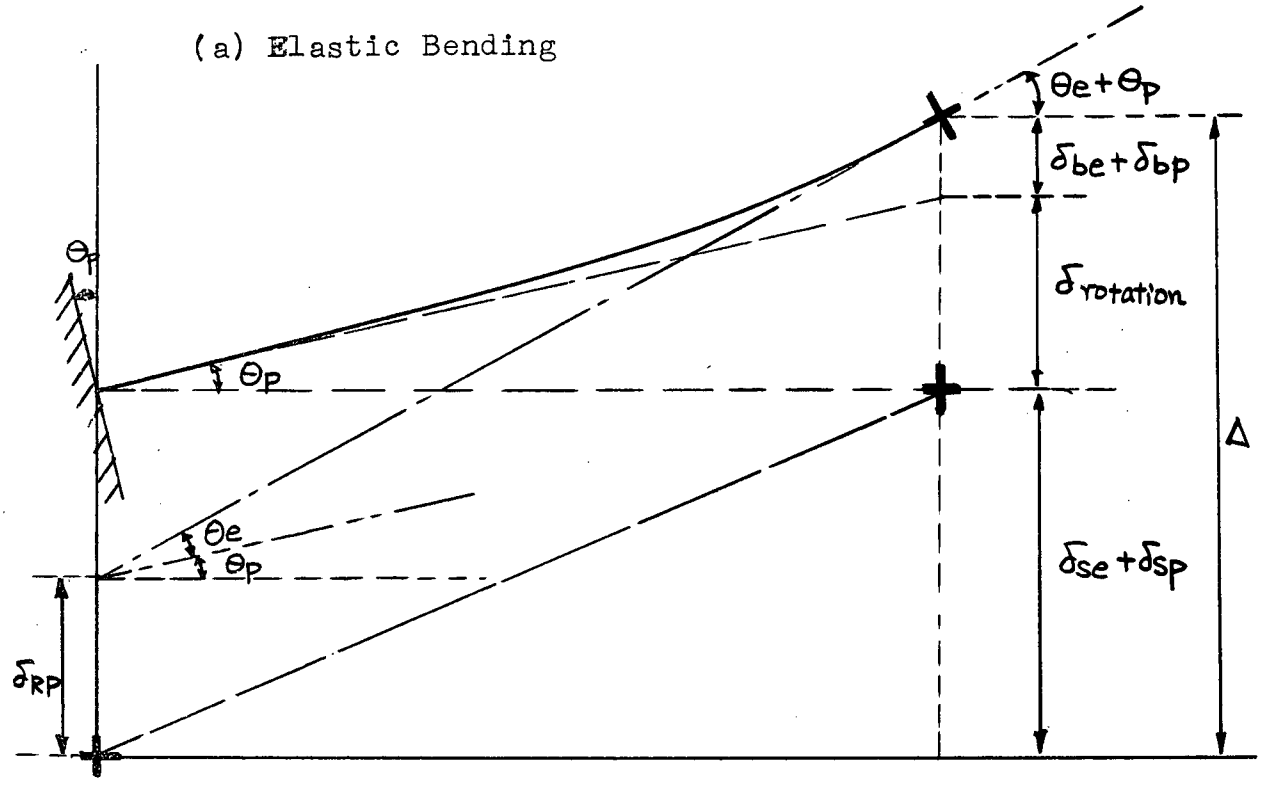

(b) Plastic Bending

$$\theta_P = \frac{\Delta - \delta_{RP}}{\text{Gage Length of Rotation Gage}} - \theta_e$$

NOTATIONS: δ = Deflection θ = Angle change

Subscript e = Elastic
Subscript p = Plastic
Subscript R = Rotation gage
Subscript s = Shear
Subscript b = Bending

FIG. 8 - ANALYSIS OF ROTATION GAGE

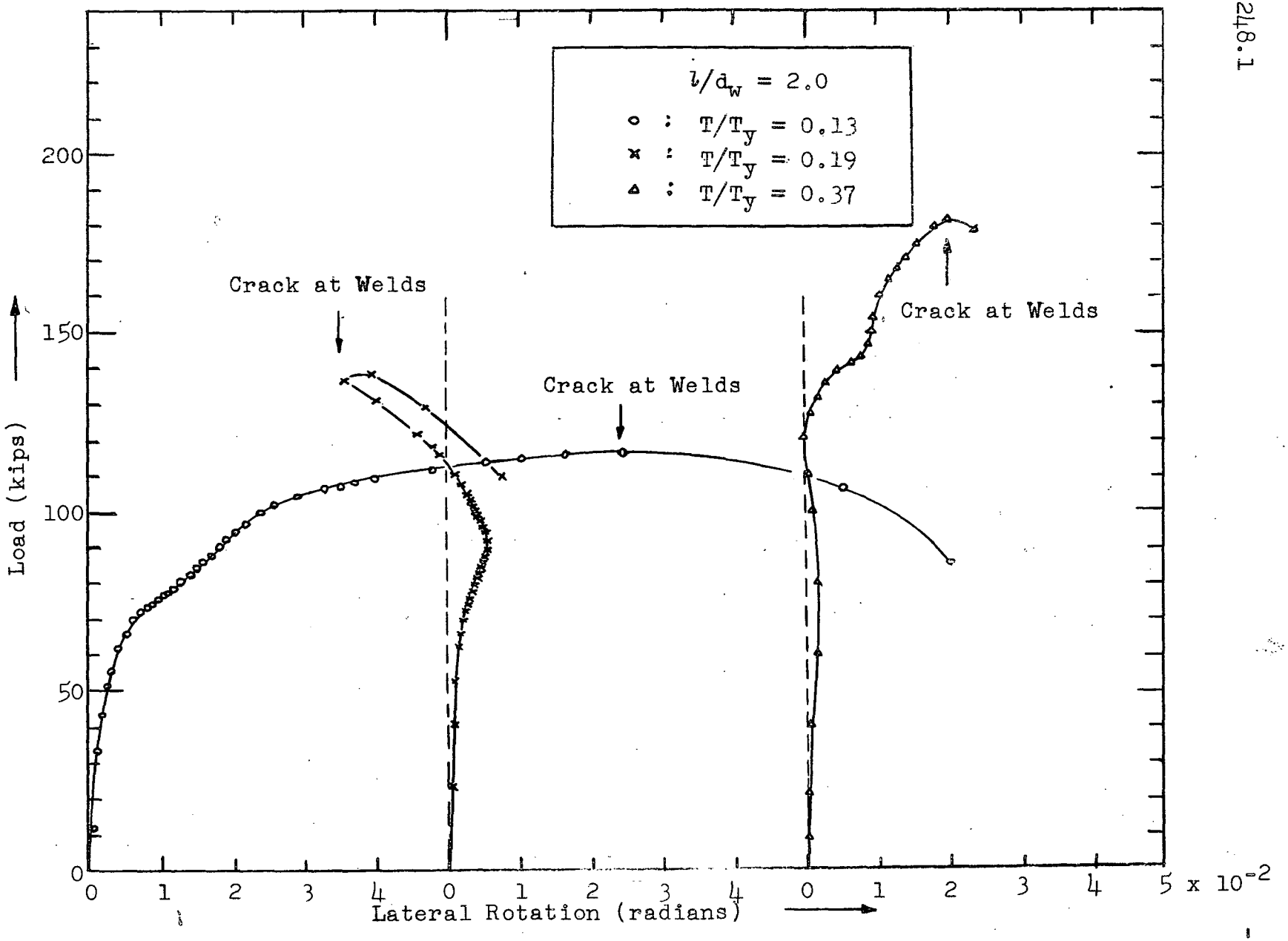

FIG. 9 - LATERAL ROTATION

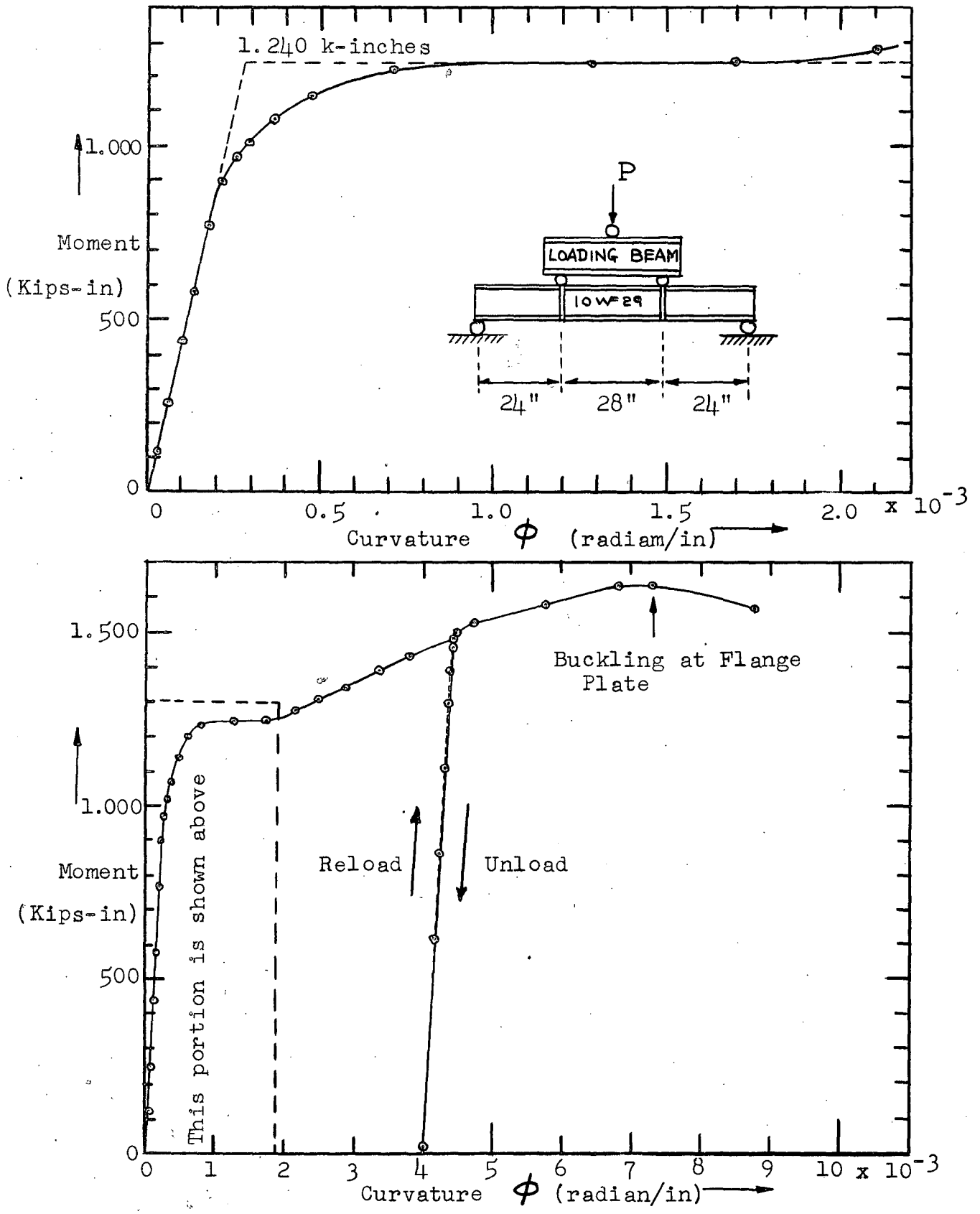

FIG. 10 - MOMENT-CURVATURE CURVE OF THE CONTROL BEAM (UNIFORM MOMENT)

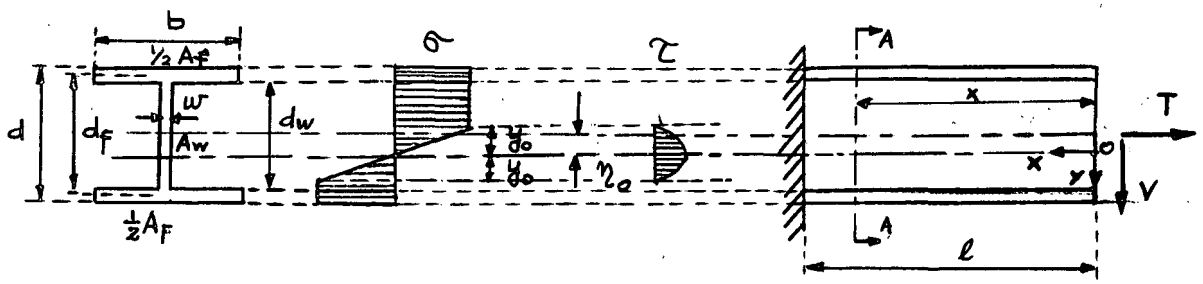

FIG. 11 - ASSUMED STRESS DISTRIBUTION IN WF SHAPES

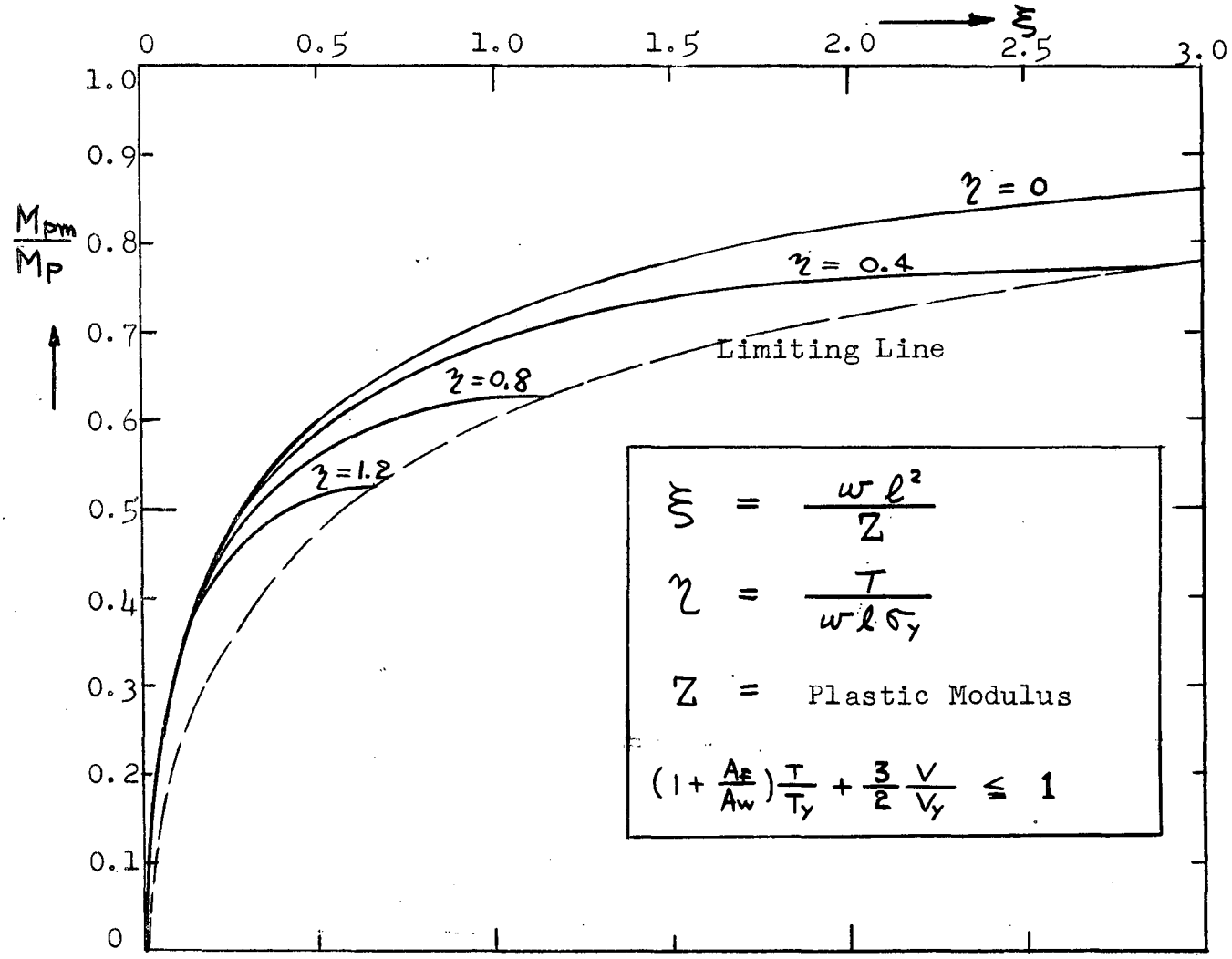

FIG. 12 - INTERACTION CURVES BETWEEN MOMENT, SHEAR AND AXIAL FORCES (NEUTRAL AXIS IN WEB)

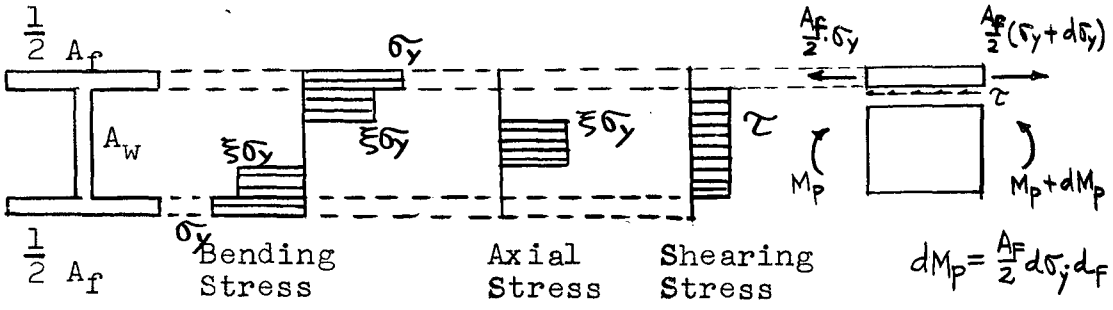

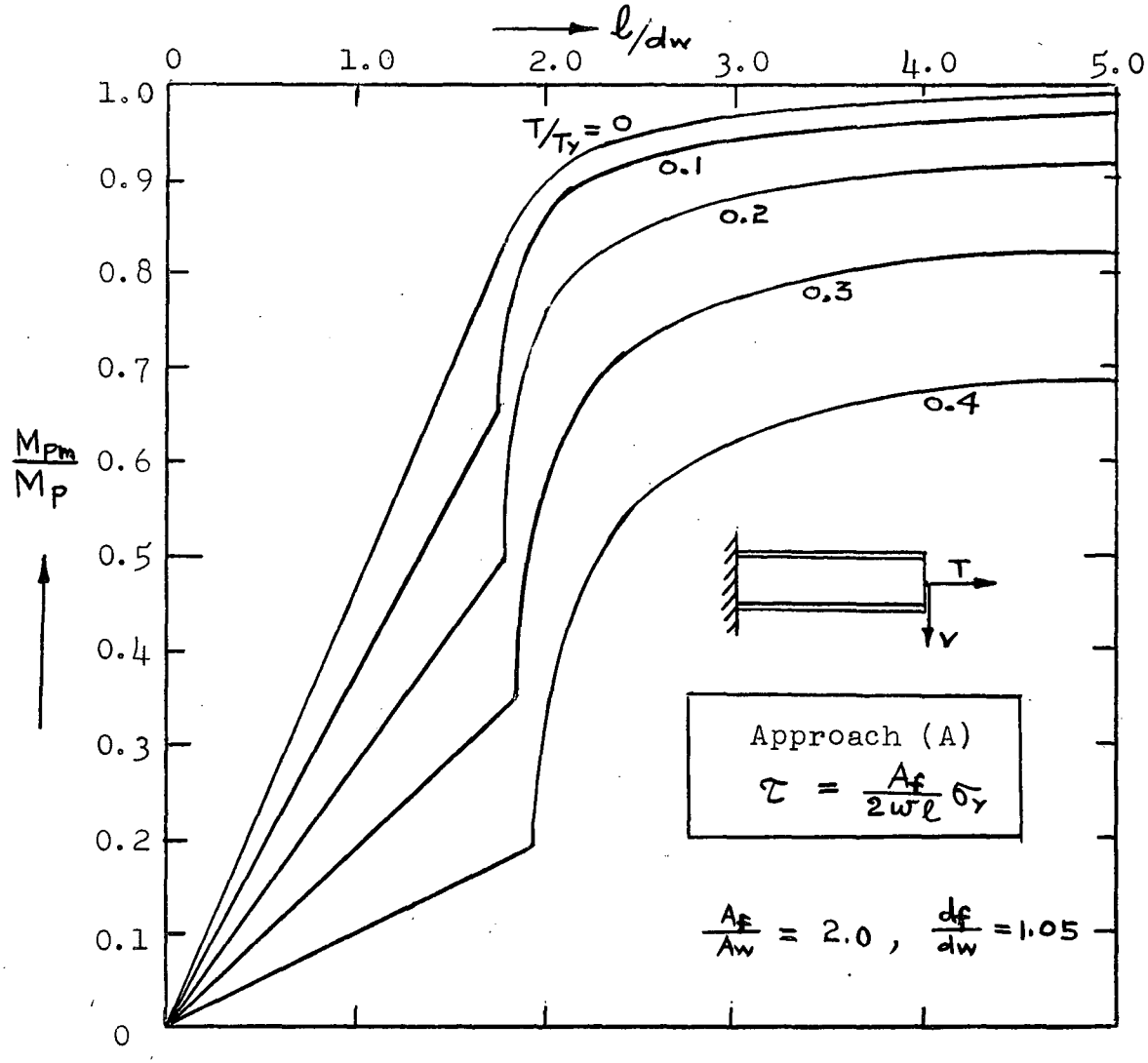

FIG. 13 - INTERACTION CURVES BETWEEN MOMENT, SHEAR AND AXIAL FORCES--APPROACH (A)--

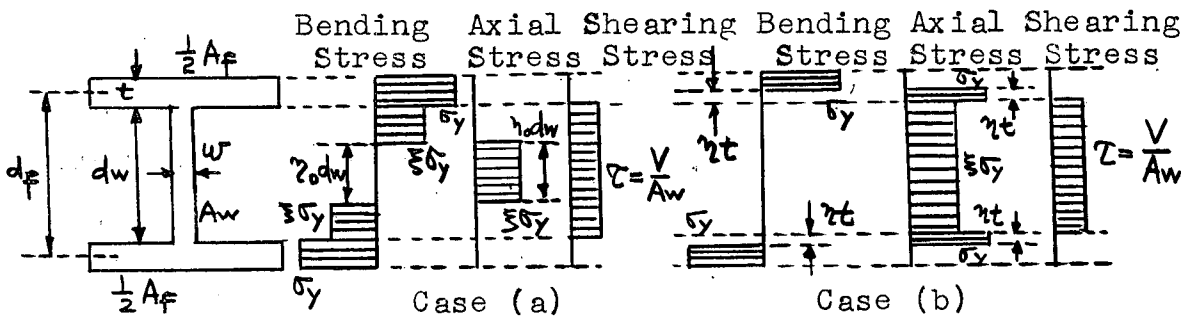

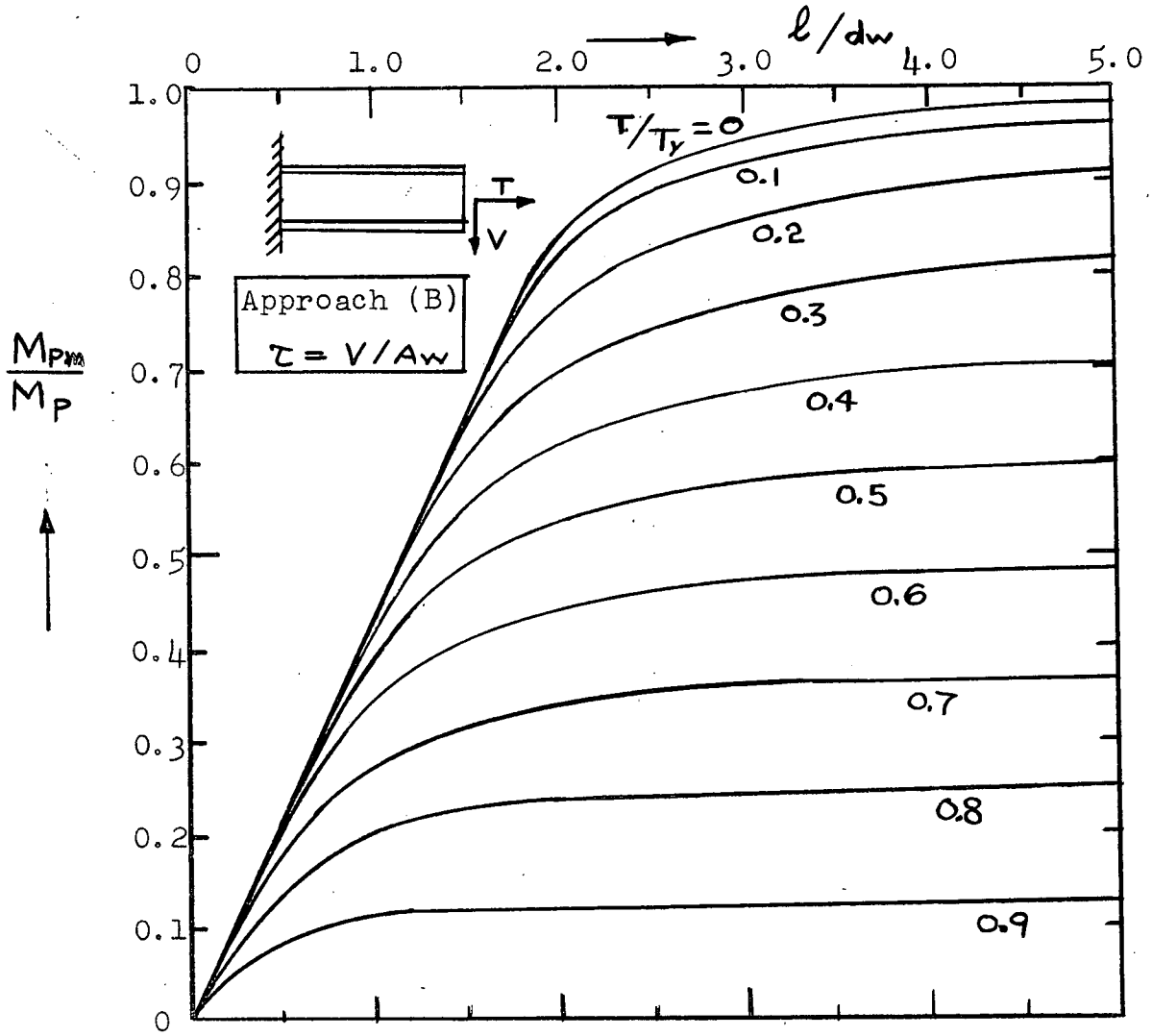

FIG. 14 - INTERACTION CURVES BETWEEN MOMENT, SHEAR AND AXIAL FORCES--APPROACH (B)--

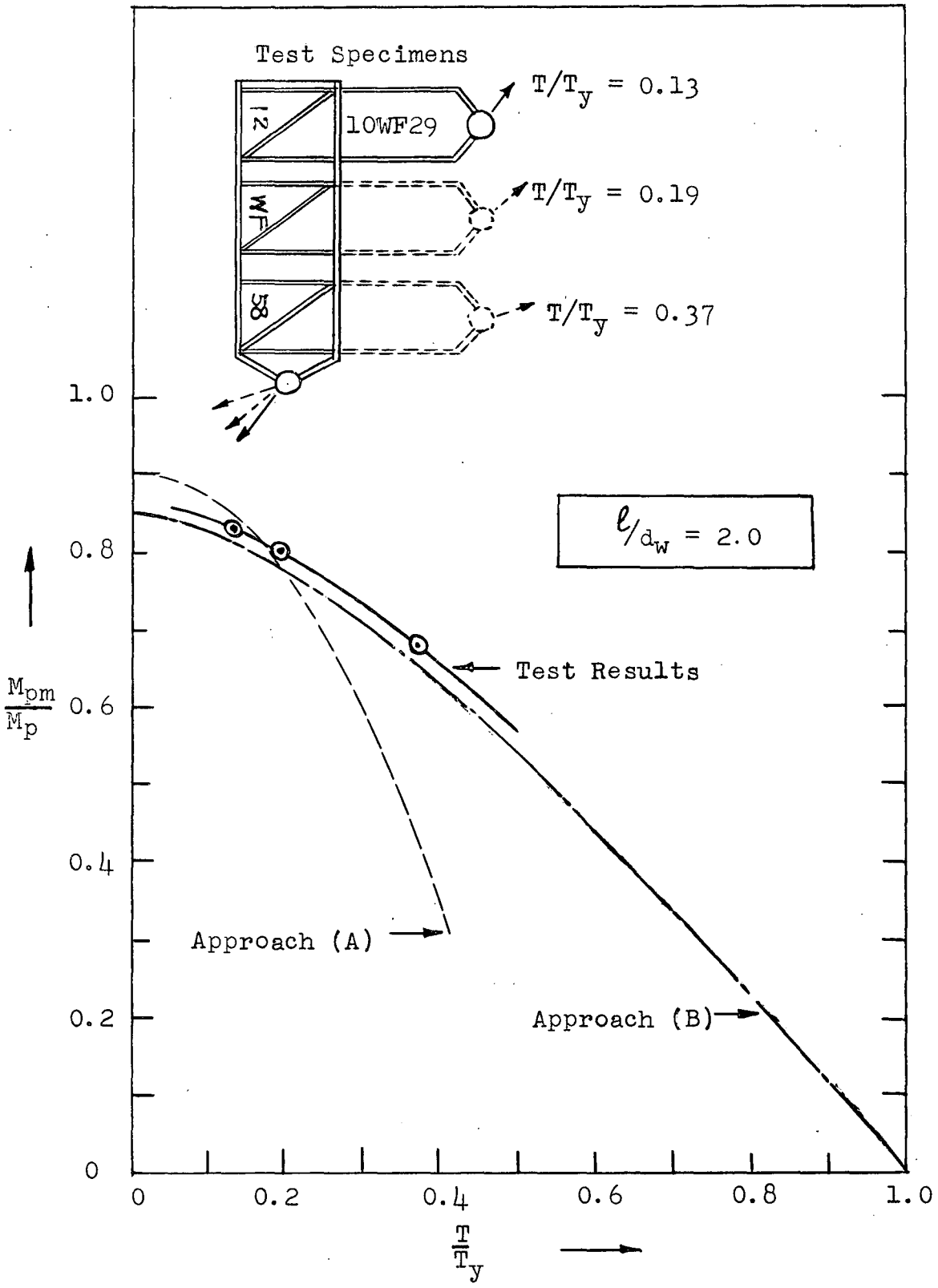

FIG. 15 - REDUCTION OF PLASTIC MOMENT DUE TO SHEAR AND AXIAL FORCE

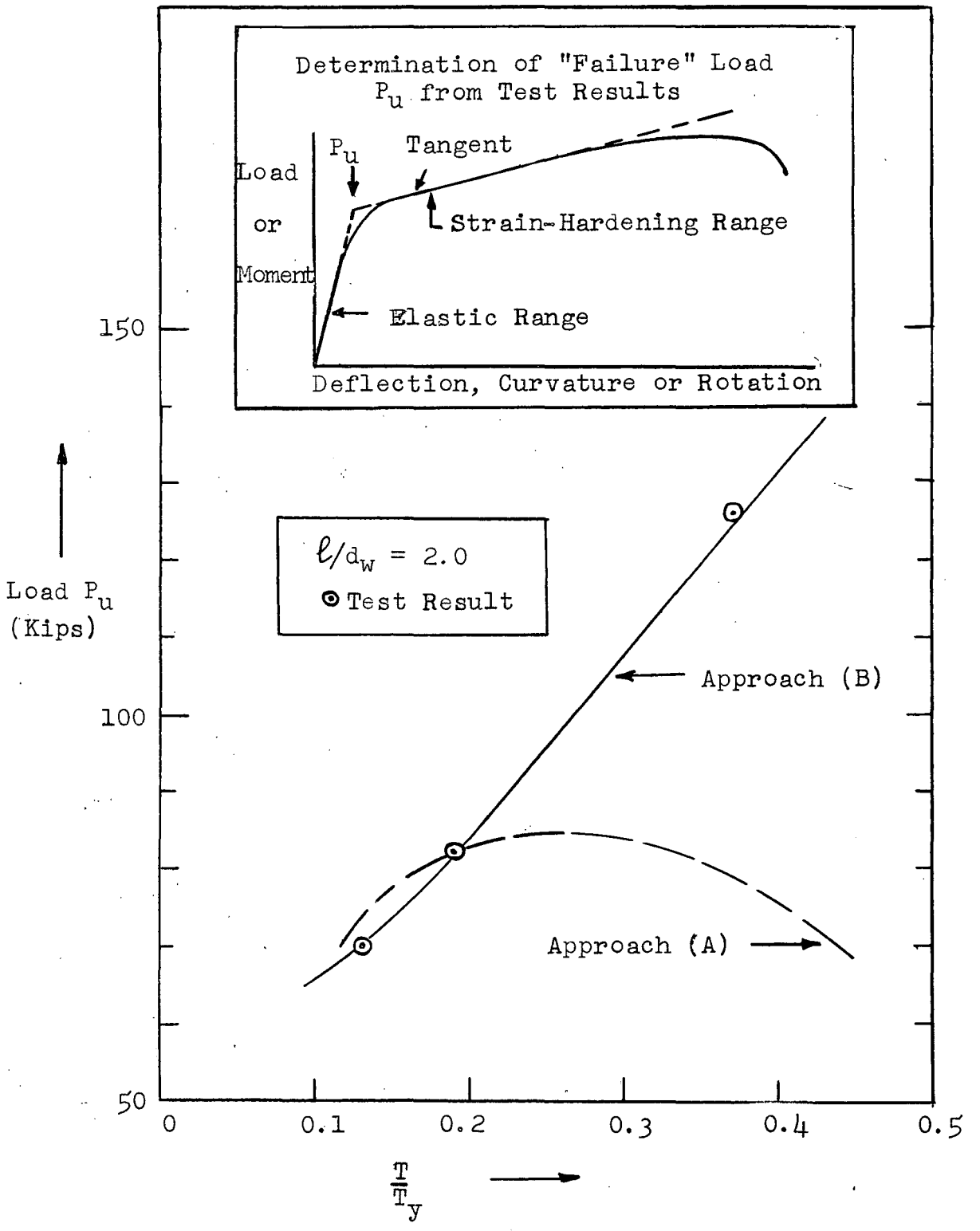

FIG. 16 - "FAILURE" LOAD P_u OF WF-BEAM UNDER MOMENT, SHEAR AND AXIAL FORCE

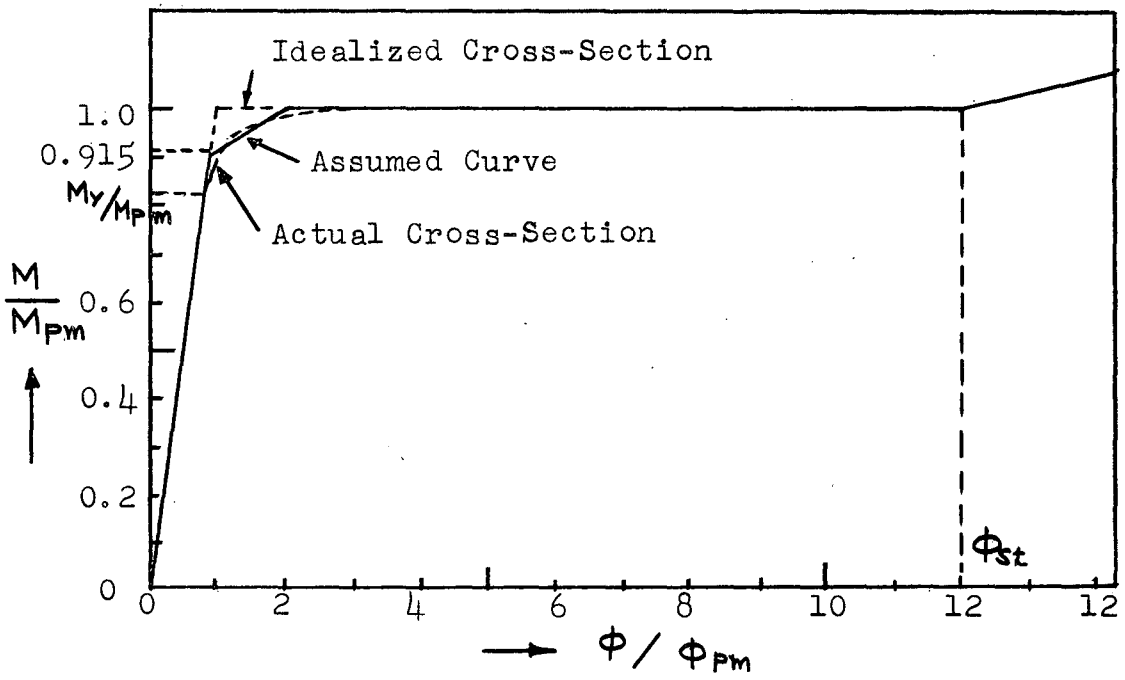

FIG. 17 (a) - ASSUMED MOMENT-CURVATURE CURVE

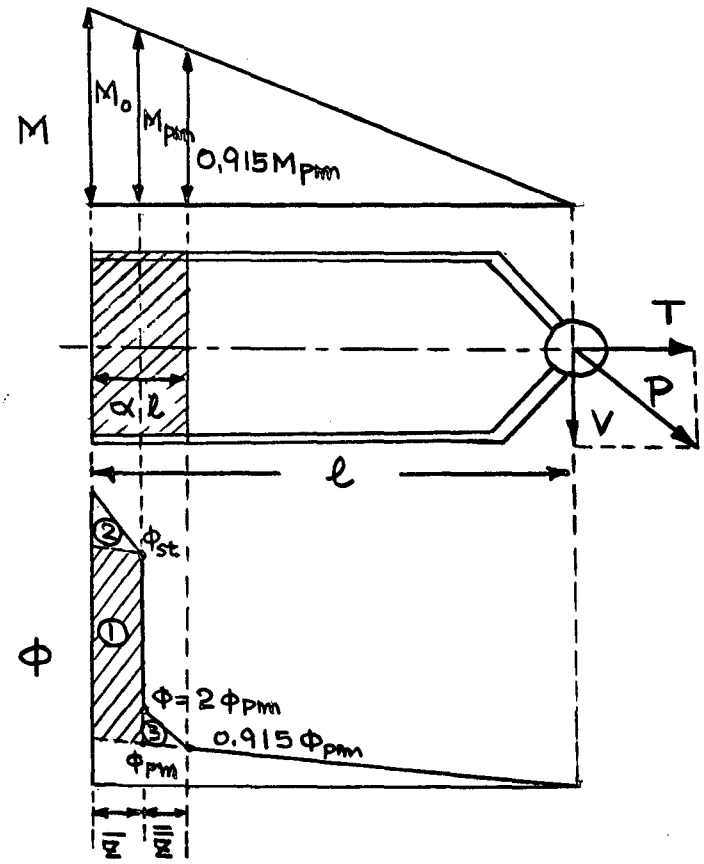

FIG. 17 (b) - ASSUMED CURVATURE DIAGRAM

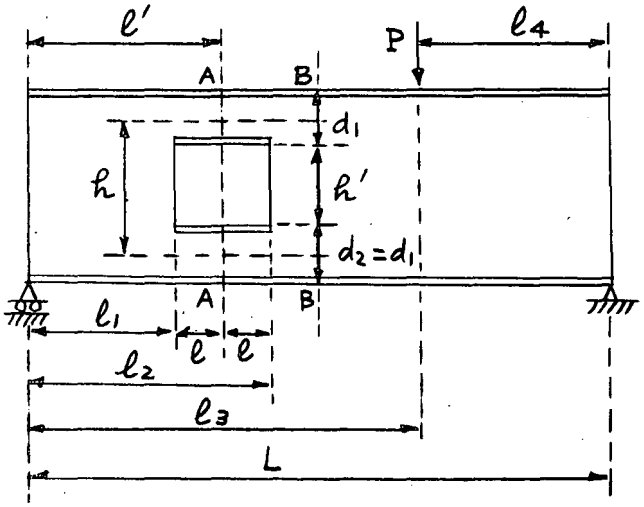

FIG. 18 (a) - BEAM WITH CUTOUT

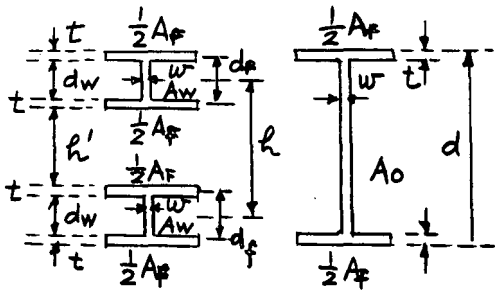

FIG. 18 (d) - CROSS-SECTION AT A-A AND B-B

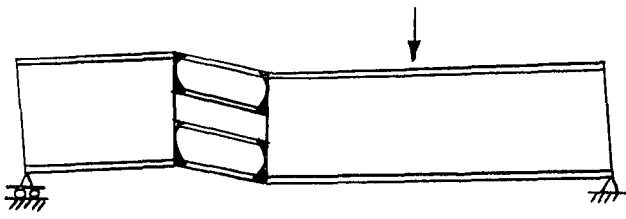

FIG. 18 (b) - MECHANISM I

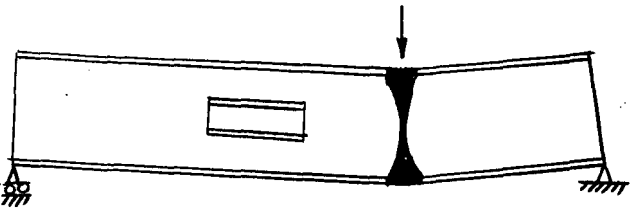

FIG. 18 (c) - MECHANISM II

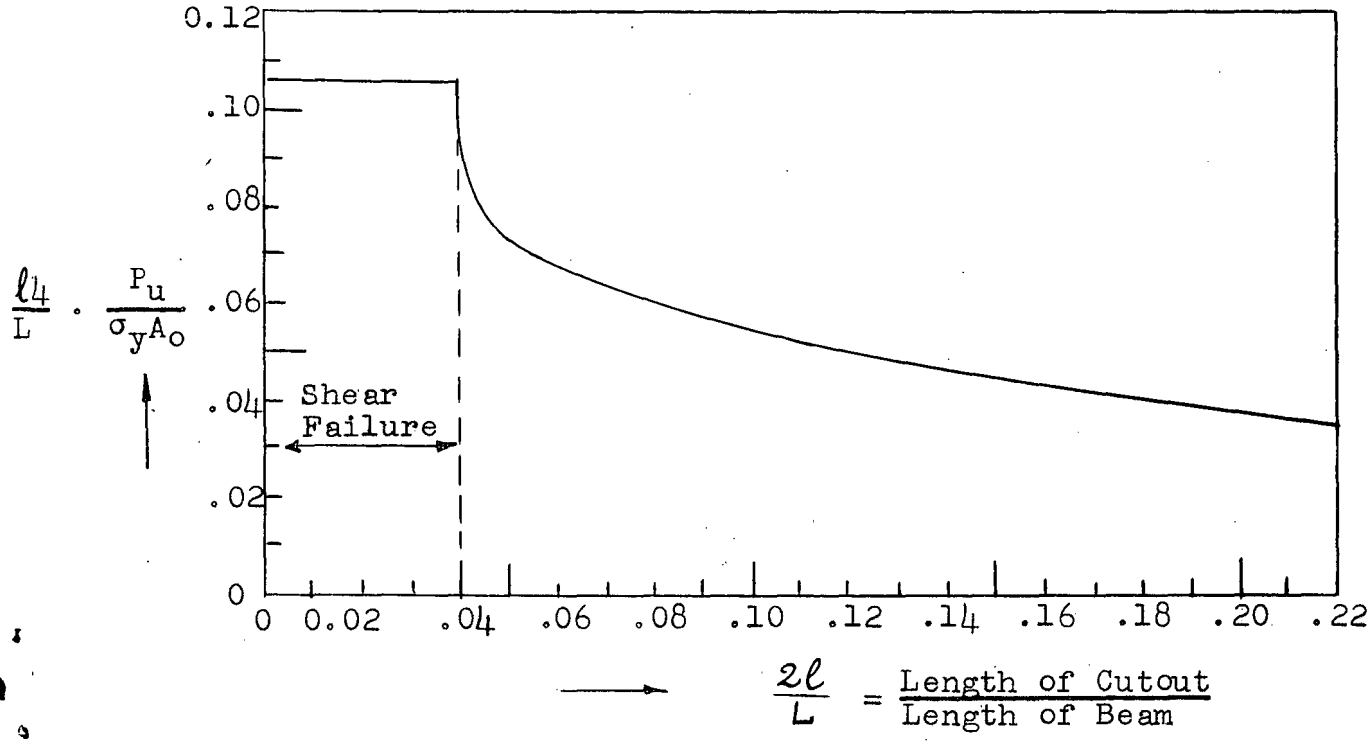

FIG. 18 (e) - ULTIMATE LOAD OF BUILT-UP BEAM WITH CUTOUT